Review

Review of electrochemical studies of complexes containing the Fe_2S_2 core characteristic of [FeFe]-hydrogenases including catalysis by these complexes of the reduction of acids to form dihydrogen

Greg A.N. Felton, Charles A. Mebi, Benjamin J. Petro, Aaron K. Vannucci, Dennis H. Evans *, Richard S. Glass *, Dennis L. Lichtenberger *

Department of Chemistry, The University of Arizona, 1306 East University Boulevard, Tucson, AZ 85721, USA

ABSTRACT

This article reviews published literature on the electrochemical reduction and oxidation of complexes containing the Fe_2S_2 core characteristic of the active site of [FeFe]-hydrogenases. Correlations between reduction and oxidation potentials and molecular structure are developed and presented. In cases where the complexes have been studied with regard to their ability to catalyze the reduction of acids to give dihydrogen, the overpotentials for such catalyzed reduction are presented and an attempt is made to estimate, at least qualitatively, the efficiency of such catalysis.

© 2009 Elsevier B.V. All rights reserved.

Contents

---

* Corresponding authors. Tel.: +1 520 626 0318; fax: +1 520 621 8407 (D.H. Evans).
  E-mail address: dhevans@email.arizona.edu (D.H. Evans).

1. Introduction

Since it was shown [1] that the active site of [FeFe]-hydrogenases contains a "butterfly" Fe_2S_2 group at its center (see below) much attention has been directed to the synthesis and characterization of bioinspired complexes that resemble this active site structure. The interest here is centered on the attractive possibility that new catalysts for hydrogen production, based on inexpensive metals such as iron, might be developed and that such catalysts might pave the way for the development of the hydrogen energy economy.
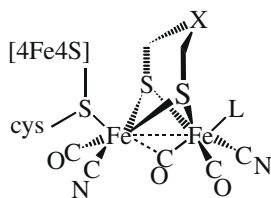
The source of reducing equivalents for converting protons to dihydrogen could be chemical reductants (e.g., biomass), photochemistry (solar) or electrochemistry, where the needed electrons come from an electrode. However, it is the last of these that comprises the simplest and most convenient means of testing the efficacy of newly synthesized catalysts. Consequently, numerous reports have appeared concerning the electrochemical reactions of such complexes both in the absence and presence of acids.

In this review, we will summarize these studies which have been conducted on almost 250 synthetic catalyst candidates.[1]

2. Methodology

In this section we will explain the methodology of extracting data from the literature, expressing the data in a consistent format and interpreting the data.

2.1. Potentials

Almost all of the potentials reported have been obtained by cyclic voltammetry. In this technique, the potential of the electrode is moved from a value where no reaction occurs to one where reduction or oxidation of the solute occurs followed by a return scan to the initial potential. The cyclic voltammogram is a plot of current vs. the applied potential and it generally displays a peak in the current-potential plot on both the forward and reverse scans. The magnitude of the peak is called the peak current and the position of the peak along the potential axis is called the peak potential. It is customary to identify two different kinds of reversibility in cyclic voltammetry. The first is chemical reversibility which is indicated by equal peak currents for the forward and reverse scans with the reverse peak current being measured from the extension of the current on the forward scan. This simply means that the electrogenerated product is stable on the time scale of the voltammogram. The second type of reversibility is electrochemical reversibility which means that the heterogeneous electron-transfer reaction is fast in relation to the time scale of the voltammogram. Electrochemical reversibility is indicated by peak potentials that are separated by $\sim$58 mV (298 K), i.e., $\Delta E_p = E_{pa} - E_{pc} = 58$ mV, where E_{pa} and E_{pc} are the anodic and cathodic peak potentials, respectively. This relationship pertains to a one-elec-

tron reaction. The situation with a two-electron process is more complicated with ΔE_p depending upon the relative values of the two individual one-electron standard potentials, $E°_1$ and $E°_2$.

For reactions that are both chemically and electrochemically reversible, the half-wave potential, $E_{1/2}$, is obtained with good accuracy by equating it to the average of the peak potentials, $E_{1/2} = (E_{pc} + E_{pa})/2$. For our purposes this is sufficiently valid even in cases where incomplete chemical reversibility (peak on reverse scan is too small) so long as a peak is clearly discernible. Also, this relationship is reasonably accurate in cases of incomplete electrochemical reversibility ($\Delta E_p > 58$ mV) but it probably should not be applied for cases where the peak separation exceeds $\sim$80 mV.

The reason that the half-wave potential is important is that it is almost identical to the standard potential of the reaction. For $O + e^- \rightleftharpoons R$, $E_{1/2} = E° + (RT/2F)\ln(D_R/D_O)$, where $E°$ is the standard potential and D_O and D_R are the diffusion coefficients of O and R, respectively. (Here we will not distinguish between $E°$, which pertains to infinite dilution, and $E°'$, the formal potential which is what is measured with a given concentration of electrolyte). The diffusion coefficients are usually very similar, within 5–40% of one another, leading to $E_{1/2}$ differing from $E°$ by $\leqslant$4 mV. Since $\Delta G° = -nFE°$ (where n is the number of electrons in the cell reaction, in this case one), the standard potential reflects the free energy difference between O and R, valuable information for characterization of the metal complexes. In reality, $\Delta G°$ will depend upon the reference electrode. That is, $\Delta G°$ actually corresponds to the free energy change of the entire cell reaction, $O + Fc \rightleftharpoons R + Fc^+$ when using the ferrocene redox couple as a reference. (For a presentation of these and other characteristics of cyclic voltammetry see [2]).

In the literature being reviewed in the present paper, there are a few cases in which chemical reversibility has been observed and authors have reported values of $E_{1/2}$ or $E°$. For reasons mentioned above, $E_{1/2}$ will be reported as $E°$. Actually, many reactions, reported as being irreversible, do show a significant peak on the reverse scan so that $E°$ could be estimated. However, we will tabulate the peak potentials for all cases reported as being irreversible. The peak potential is not the same as the standard potential but is related to it. For very simple cases, for example, a totally irreversible electron-transfer reaction or an irreversible chemical reaction following an initial reversible electron-transfer, the standard potential can be extracted from the peak potential with the help of kinetic constants. However, such detailed analyses are infrequently encountered in this literature so the E_p-values can only be taken as approximate measures of the tendency of the reactant to accept or give up electrons. However, as mentioned above, when a peak is discernible on the return scan, the standard potential is close to the peak potential.

In most cases, authors explicitly report peak potentials as this is the most frequently measured quantity in cyclic voltammetry. However, in some cases terms such as "oxidation potential", "reduction potential" or just "potential" are used. When such terms are used, we have assumed that the authors mean "peak potential".

Measured values of $E°$ are independent of the material used in the working electrode but irreversible peak potentials can depend on the nature and condition of the working electrode, the supporting electrolyte, scan rate and other factors. Fortunately, almost all of the reviewed research has used glassy carbon working electrodes. Another factor affecting measured potentials is the effect of solution resistance. Though inspection of published voltammograms reveals that significant resistance effects are present in some cases, these have been ignored. In a few cases, the effects of solution resistance have been removed during data analysis and those cases will be identified when encountered.

Seven reports of E_{pc} for $(\mu\text{-}S(CH_2)_3S)Fe_2(CO)_6$ in acetonitrile have been identified (Compound **36**, Table 3.1). The measurement conditions were nearly identical though there was some variation in the scan rate. The mean of these seven values was -1.66 V vs.

---

[1] During the late stages of preparation of this review, another review covering some of the same topics appeared [99].

ferrocene with a standard deviation of 0.06 V. This result provides a rough idea of the degree of consistency found in the literature and the uncertainties involved in translating all values to the ferrocene scale (cf. Section 2.2).

Many complexes show more than one reduction or oxidation peak. As the major purpose of the review is to correlate structure with the tendency to accept or give up electrons, only the first reduction and the first oxidation process are reported. Processes occurring at subsequent peaks are often of an unknown nature. However, in cases where a reasonable explication of a second reduction or oxidation process has been provided, the data will be reported.

2.2. Reference electrode

Many authors follow the procedure recommended by IUPAC [3,4] by which the potentials are referenced to the standard potential of the $(\eta^5\text{-}C_5H_5)_2Fe^+/(\eta^5\text{-}C_5H_5)_2Fe$ couple measured in the solvent being used. (In this paper we will abbreviate $(\eta^5\text{-}C_5H_5)_2Fe^+/(\eta^5\text{-}C_5H_5)_2Fe$ as Fc^+/Fc and sometimes call it the "ferrocene potential" or simply "ferrocene"). This can be done in two ways. In cases where there is no danger of interaction between ferrocene and the compound being studied, the ferrocene can be added as an internal standard and a voltammogram containing peaks for both ferrocene and the compound being studied is recorded from which the potentials vs. the Fc^+/Fc potential can be readily measured. In other cases a practical laboratory reference electrode is used for studies of the compound and in separate experiments with ferrocene, the Fc^+/Fc standard potential is measured vs. the practical laboratory reference electrode. Finally, all potentials are expressed vs. the ferrocene potential.

In some cases it is not clear that authors are using the standard potential of ferrocene as a reference, as estimated from the mean of its anodic and cathodic peak potentials (see above). It appears that occasionally one of the peak potentials of the ferrocene couple is being used as reference. Fortunately, this only introduces an error of about 30 mV. Other authors simply report potentials vs. the reference electrode used in the study. A common example of such a reference electrode is a silver wire in contact with 0.010 M $AgNO_3$ in acetonitrile (usually also containing the supporting electrolyte), abbreviated AgRE. Long experience with this reference electrode shows that its potential is not extremely stable nor reproducible from one worker to the next. What is used in this review is an average value of the ferrocene standard potential of +0.080 V vs. AgRE. A Nernst correction is applied when 0.0010 M $AgNO_3$ is used, i.e., the ferrocene standard potential is +0.139 V vs. this AgRE.

Other authors report using the SCE, saturated calomel electrode. There is not much ambiguity about this electrode as it is always comprised of Hg, Hg_2Cl_2 and saturated aqueous KCl. We have measured the ferrocene standard potential in acetonitrile vs. the SCE and found it to be +0.393 V vs. SCE at 298 K [5]. In this review, this value was used to express the potentials reported vs. SCE to values vs. ferrocene.

The final reference electrode that is frequently employed is the Ag/AgCl electrode whose most common manifestation involves Ag, AgCl and saturated aqueous KCl. As its potential is +0.197 V vs. NHE and SCE is +0.241 V vs. NHE, then Fc^+/Fc is +0.393 + (0.241 − 0.197) =

+0.437 V vs. this Ag/AgCl reference [6]. In a few cases, authors do not report the nature of the Ag/AgCl reference electrode (for example, the chloride concentration is not reported). The compilers were forced to assume that saturated KCl was used, an assumption that, if incorrect, would lead to errors of probably 30 mV or less.

In a few cases, [7–9] potentials were said to have been reported vs. aqueous NHE. Correspondence with the senior author revealed that 0.400 V should be subtracted from these potentials to obtain values referenced to Fc^+/Fc in acetonitrile [10]. All of these values are summarized in Table 2.1.

Other solvents such as DMF, THF and CH_2Cl_2 have been used in studies of the complexes reviewed in this work. Except as otherwise noted, the potentials measured in these solvents have been referenced to the standard potential of ferrocene in acetonitrile.

2.3. Overpotential

Frequently complexes are tested for their ability to catalyze the reduction of acids to form dihydrogen. Data concerning this catalysis is tabulated in Table 4.5. Successful complexes should accomplish this with low overpotential, defined for the present purposes as the difference between the standard potential for reduction of the acid and the potential where the catalytic reduction occurs. The standard potential for reduction of the acid corresponds to the half reaction:

$$2HA + 2e^- \rightleftharpoons H_2 + 2A^-$$
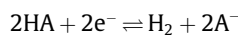
It has been pointed out [11] that this standard potential, E°_{HA}, can be computed for any acid whose pK_a is known in the solvent being used. This is particularly valuable for *N,N*-dimethylformamide, dimethylsulfoxide and acetonitrile for which pK_a-values of many acids are known. Though we have promoted the use of the potential at half the catalytic peak height as the potential where catalysis occurs [12] such potentials are difficult to estimate from published voltammograms so in this review we will use the peak potential of the catalytic peak.

Catalysis can occur at the first reduction peak of the catalyst or at more negative potentials where the catalyst itself may or may not exhibit a reduction peak. We will attempt to report the catalysis and the overpotential for all peaks where the catalysis is significant.

2.4. Catalytic efficiency

The second major attribute of a good catalyst is high efficiency, exhibited in the case of electrochemistry by large catalytic currents for given concentrations of catalyst and acid. In chemical catalysis and biochemistry the preferred measure of efficiency is turnover frequency. However, turnover frequency has not turned out to be a generally applicable concept in voltammetry. So, we are left with the catalytic current as the only measure of efficiency. In this review a qualitative description of efficiency will be denoted by the descriptors strong (S), medium (M) or weak (W). To the extent possible, the evaluation is based on comparable conditions: concentration of catalyst, concentration of acid, scan rate, etc. Basically, the ratio of the catalytic current, i_{cat}, to the current for reduction of the catalyst in the absence of acid, i_d, is examined. This ratio is divided by the ratio of the acid concentration, C_{HA}, to the catalyst concentration, C_{cat}. Thus, the catalytic efficiency, *C.E.*, is given by

$$C.E. = \frac{i_{cat}/i_d}{C_{HA}/C_{cat}}$$

When maximum efficiency is obtained, the catalytic current will be controlled by the diffusion of HA to the electrode so it should be

Table 2.1
Corrections used to convert potentials vs. various reference electrodes to potentials vs. ferrocene in acetonitrile.

Reference electrode	Correction (V)
E vs. Fc⁺/Fc in CH₃CN = E vs. reference + correction	
Ag/0.010 M $AgNO_3$ in CH_3CN	−0.080
Ag/0.0010 M $AgNO_3$ in CH_3CN	−0.139
SCE, $Hg/Hg_2Cl_2(s)$, KCl(s), aq.	−0.393
Ag/AgCl(s), KCl(s), aq.	−0.437
"NHE" [10]	−0.400

proportional to C_{HA}. If i_d is related to C_{cat} by the same constant of proportionality, C.E. will equal unity at maximum efficiency. At the other extreme, when there is no catalysis, i_{cat} equals 0 and so does C.E. Thus C.E. should vary between 0 and 1. Arbitrarily, we have assigned W for 0 < C.E. < 0.25, M for 0.25 < C.E. < 0.75 and S for C.E. > 0.75. This treatment is not exact but was chosen as a reasonable means of classifying the catalytic efficiency. (For cases where the reduction of the catalyst is known to be a two-electron process, i_d was divided by two).

There is a complicating factor that must be mentioned: the direct reduction of the acid at the electrode must be considered. At any potential where the acid may be reduced catalytically, it must also be capable of being reduced directly at the electrode.

For the glassy carbon electrodes usually employed, the direct reduction of acetic acid becomes important around −2.2 V vs. ferrocene [11]. For stronger acids, the direct reduction occurs at even less negative potentials. The use of mercury or gold-amalgam electrodes brings about a larger overpotential for direct reduction but the strong interaction of sulfur compounds with mercury can render these electrodes useless for some complexes. In many cases, authors report the extent of direct reduction, measured with the acid in the absence of catalyst. However, in other cases such measurements are not reported. Whenever it would appear that direct reduction is contributing significantly to the catalytic current, the entry is denoted by "dr" in the tabulated data (Table 3.1).
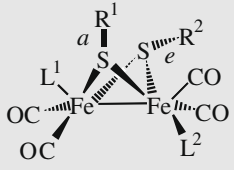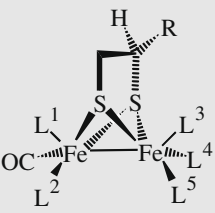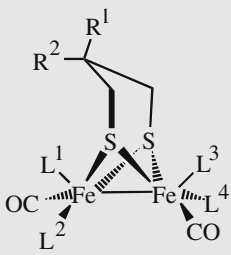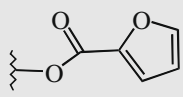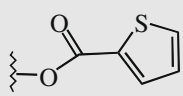
Table 3.1
Electrochemical data.[a]

Definition of axial (a) and equatorial (e) positions. In most cases the isomeric identity has not been reported.

Compounds	R^1	R^2	All CO ligands except	Solvent	E_{pc}	E_{pa}	Reference
1	Me	Me		PC[b]	−1.55	+0.81	[13]
2	C_6H_5	C_6H_5			−1.37	+0.59	
3	Me	Me	$L^1 = L^2 = PMe_3$		−2.59	+0.71	
4	e-Me	e-Me		DMF	−1.64[c]		[14]
5	e-Et	e-Et			−1.60[c]		
6	a-Et	e-Et			−1.58[c]		
7	Et	Et		THF	−1.69		[15]
				CH_3CN	−1.71	+0.78	[8]
8	Et	Et	$L^1 = L^2 = PMe_3$ (both apical)		−2.31	−0.13	
9	t-Bu	$MeSCH_2$		CH_3CN	−1.71	~+0.5	[16]
10	$HOOCCH_2CH_2$	$HOOCCH_2CH_2$		CH_3CN	−1.73		[17]
11	2-$RCONHC_6H_4$	2-$RCONHC_6H_4$		CH_3CN	−1.29	+0.74	[18]
	R = Me	R = Me					
12	R = CF_3	R = CF_3			−1.22	+0.88	
13	R = C_6H_5	R = C_6H_5			−1.24	+0.75	
14	R = 4-FC_6H_4	R = 4-FC_6H_4			−1.19	+0.77	
15	C_6H_5	C_6H_5		CH_3CN	−1.44	+0.81	[19]
16	2-$MeOC_6H_4$	2-$MeOC_6H_4$			−1.55	+0.73	
17	4-$MeOC_6H_4$	4-$MeOC_6H_4$			−1.51	+0.93	
18	4-ClC_6H_4	4-ClC_6H_4			−1.35	+0.79	
19	2-$MeOC_6H_4$	2-$MeOC_6H_4$	$L^1 = L^2 = PMe_3$		−2.08	−0.23	
20	R^1, R^2 = 1,2-xylenediyl			CH_3CN	−1.56	+0.80	[8]
				CH_2Cl_2	−1.68[d] ($E°$)		[20]
21	R^1, R^2 = $H_2C(CH_2OCH_2)_nCH_2$ $n = 1$			CH_3CN	−1.44 ($E°$)	+0.54	[21]
22	$n = 2$				−1.56 ($E°$)	+0.58	
23	$n = 3$				−1.54 ($E°$)	+0.59	
24	$n = 4$				−1.56 ($E°$)	+0.64	

Compounds	R	All CO ligands except	Solvent	E_{pc}	E_{pa}	Reference
25	H		DMF	−1.56[e]		[14]
26			THF	−1.74		[15]
27		L^1, $L^2 = L^3$, L^4 = cis-$Ph_2PCH=CHPPh_2$	CH_2Cl_2		−0.612 ($E°$)[f]	[22]
28		$L^1 = NO^+$; $L^2 = PMe_3$	CH_2Cl_2	−0.80		[23]
29		$L^1 = NO^+$; $L^2 = L^3 = PMe_3$		−1.11		
30		L^1, L^2 = cis-$Ph_2PCH=CHPPh_2$	CH_2Cl_2		−0.018 ($E°$)	[24]
31		L^1, L^2 = cis-$Ph_2PCH=CHPPh_2$; L^3 = $P(iPr)_3$			−0.267 ($E°$)	
32		L^1, L^2 = cis-$Ph_2PCH=CHPPh_2$; L^3 = PMe_3			−0.417 ($E°$)	
33		L^1, $L^2 = L^3$, L^4 = cis-$Ph_2PCH=CHPPh_2$			−0.612 ($E°$)	
34	$HOCH_2$		CH_3CN	−1.67	+0.9	[25]
35		$L^2 = L^5 = CN^-$		−2.75	−0.47	

Table 3.1 (*continued*)

Compounds	R^1	R^2	All CO ligands except	Solvent	E_{pc}	E_{pa}	Reference
36	H	H		CH$_3$CN	−1.65	+0.74	[26]
				CH$_3$CN	−1.74	+0.74	[7,8]
				CH$_3$CN	−1.67		[27]
				CH$_3$CN	−1.67	+0.82	[28]
				CH$_3$CN	−1.71	+0.76	[25]
				CH$_3$CN	−1.59	+0.82	[29]
				CH$_3$CN		+0.90	[30]
				CH$_3$CN	−1.61 $(E°_1)^g$		[31]
				DMF	−1.56		[14]
				THF	−1.68		[29]
					−1.59		[32]
37	COOH	H		CH$_3$CN	−1.64		[17]
38	COOH	H	$L^2 = L^4 = PMe_3$		−2.42		
39	C(O)NHPh	H			−1.67		
40	[furan-2-carboxylate ester group]	H		CH$_3$CN	−1.58	+0.85	[33]
41	[thiophene-2-carboxylate ester group]	H			−1.59	+0.84	
42	Me	Me		CH$_3$CN	−1.61	+0.73	[34]
43	Me	Me	$L^1 = PPh_3$		−1.79	+0.69	
44	Et	Et			−1.67	+0.82	
45	*n*-Bu	Me			−1.64	+0.78	
45a	Me	Me	$L^2 = L^4 = PMe_3$	CH$_2$Cl$_2$		−0.34	[94]
46	Ru-ligand 1	H		CH$_3$CN	−1.58	+0.8	[35]
47	H	H	$L^1 = PMe_3$	CH$_3$CN	−1.94	+0.23	[26]
48			$L^1 = PMe_2Ph$		−1.90	+0.17	
49			$L^1 = PPh_3$		−1.84	+0.18	
50			$L^1 = P(OEt)_3$		−1.81	+0.37	
51			$L^1 = PPh_2(NHCH_2CH_2NMe_2)$	CH$_3$CN	−1.874	+0.348	[36]
52			$L^1 = PPh_2(NHC_6H_4$-2-NH$_2)$		−1.859	+0.259	
53			$L^1 = PPh_2C_6H_4$-2-CH$_2$NMe$_2)$		−1.853	+0.771	
54			$L^1 = L^3 = PMe_2Ph$	CH$_3$CN	−2.30	−0.22	[26]
55			$L^1 = L^3 = P(OEt)_3$		−2.27	−0.08	
56			$L^1 = P(OMe)_3$	CH$_3$CN	−1.98	+0.37	[37]
57			$L^1 = L^3 = P(OMe)_3$		−2.30	+0.12	
58			$L^2 = L^4 = PMe_3$	CH$_3$CN	−2.31	−0.20	[38]
				CH$_3$CN	−2.25	−0.06	[7]
				CH$_3$CN	−2.37	−0.11	[30]
				CH$_3$CN	−2.30	−0.20	[29]
59			**58** protonated at Fe–Fe	CH$_3$CN	−1.39	+1.16	[38]
				CH$_3$CN	−1.50	+1.07	[7]
60			$L^1, L^2 = Ph_2PCH_2N(Me)CH_2PPh_2$	CH$_2$Cl$_2$	−2.3	−0.17	[39]
61			**60** protonated at Fe–Fe		−1.26		
60			$L^1, L^2 = Ph_2PCH_2N(Me)CH_2PPh_2$	Acetone	−2.3	−0.1	
62			**60** protonated at N		−1.9		
63			$L^1 = PMe_2Ph, L^4 = PMe_3$	CH$_3$CN	−2.20	−0.08	[40]^h
64			$L^1 = PPh_3, L^4 = PMe_3$		−2.12	+0.02	
65			$L^1 = P(c$-C$_6H_{11})_3, L^4 = PMe_3$		−2.23	−0.10	
66			$L^1 = (OEt)_3, L^4 = PMe_3$		−2.16	+0.03	
67			$L^1 = PPh_3, L^4 = PMe_2Ph$		−2.09	+0.03	
68			$L^1 = P(OEt)_3, L^4 = PMe_2Ph$		−2.17	+0.01	
69			$L^1 = PPh_3, L^3 = P(OEt)_3$		−2.06	+0.13	
70			$L^1 = P(c$-C$_6H_{11})_3, L^3 = P(OEt)_3$		−2.22	+0.06	
71			$L^1 = P(OMe)_3$	CH$_3$CN	−1.98	+0.37	[37]
72			$L^1 = L^3 = P(OMe)_3$		−2.30	+0.12	

Table 3.1 (continued)
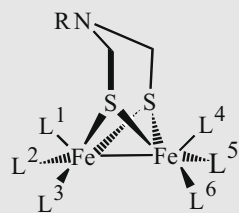
Compounds	R¹	R²	All CO ligands except	Solvent	E_{pc}	E_{pa}	Reference
73			$L^2 = P(CH_2CH_2COOH)_3$	CH$_3$CN	−2.07		[17]
74			$L^2 = PTA$	CH$_3$CN	−1.94	+0.34	[7]
75			$L^2 = L^4 = PTA$		−2.18	+0.00	
				CH$_3$CN	−2.09		[41]
76			$L^2 = L^4 = PTA-H^+$	CH$_3$CN	−1.75	+0.02	[7]
77			$L^2 = L^4 = PTA-CH_3^+$		−1.86	+0.40	
78			$L^2 = DAPTA$	CH$_3$CN	−1.83		[42]
79			$L^2 = L^4 = DAPTA$		−2.06		
80			$L^2 = DAPTA, L^4 = PTA$		−2.14		
81			$L^2 = P(pyd)_3$	CH$_3$CN	−1.98	+0.18	[43]
82			$L^3, L^4 = cis\text{-}Ph_2PCH{=}CHPPh_2$	CH$_2$Cl$_2$		−0.235 (E°)[i]	[24]
83			$L^1 = P(iPr)_3; L^3, L^4 = cis\text{-}Ph_2PCH{=}CHPPh_2$			−0.510 (E°)[i]	
84			$L^1 = PMe_3; L^3, L^4 = cis\text{-}Ph_2PCH{=}CHPPh_2$			−0.650 (E°)[i]	
85			$L^1, L^2 = L^3, L^4 = cis\text{-}Ph_2PCH{=}CHPPh_2$			−0.860 (E°)[i]	
86			$L^1, L^2 = Ph_2PCH_2CH_2PPh_2$	CH$_3$CN	−2.33	−0.17	[44]
87			$L^2 = n\text{-}PrNH_2$	CH$_3$CN	−1.80		[45]
88			$L^2 = CH_3CN$		−1.68		
89			$L^1 = SEt_2$	CH$_3$CN	−1.72		[27]
90			$L^1 = S(Et)(CH_2CH_2Cl)$		−1.76		
91			$L^1 = PhSEt$		−1.77		
92			$L^1 = S\text{-}n\text{-}Pr_2SO$		−1.65		
93			$L^1 = S\text{-}Me_2SO$		−1.68		
94			$L^1 = CNCH_3$[j]	CH$_3$CN	−1.81	+0.63	[29]
95			$L^1 = L^3 = CNCH_3$[j]		−2.08	+0.21	
96			$L^1 = CN-$		−2.17	+0.13	
97			$L^1 = CN-, L^3 = PMe_3$[k]		−2.58	−0.39	
98			Protonated at Fe–Fe[k]	CH$_3$CN	−1.57		[46]
99			Protonated at both Fe–Fe and CN$^-$[k]	CH$_3$CN	−1.42		[38]
100			$L^1 = L^4 = CN^-$	CH$_3$CN	−2.72	−0.52	[29]
101			$L^3 = NO^+, L^4 = PMe_3$	CH$_2$Cl$_2$	−0.80 (E°$_1$)[l]		[23]
102			$L^3 = NO^+, L^1 = L^4 = PMe_3$		−1.08 (E°$_1$)[m]		
103			$L^1 = IMes_2$	CH$_3$CN	−2.10	+0.11	[9,47]
104			$L^1 = IMesMe$	CH$_3$CN	−2.12	+0.23	[47]
105			$L^1 = IMe_2$		−2.01	+0.11	
				CH$_3$CN	−2.06		[48]
				CH$_3$CN	−2.08	+0.17	[30]
106			$L^1 = IMes_2, L^4 = PMe_3$	CH$_3$CN	−2.36	−0.47 (E°)	[47,49]
107			$L^1 = IMesMe, L^4 = PMe_3$		−2.52	−0.33 (E°)	
108			$L^1 = IMes_2, L^4 = PMe_3$		−2.53	−0.24 (E°)	
109			$L^1 = L^4 = IMe_2$	CH$_3$CN	−2.47		[48]
				CH$_3$CN	−2.56	−0.24	[30]
110			$L^1 = IPic_2$		−2.07	+0.11	
111			IPyMe, both N and C basal on same Fe		−2.16	−0.16	
112			CH$_2$(IMe)$_2$, both C basal on same Fe	CH$_3$CN	−2.42	−0.41	[50]
113			**112** protonated at Fe–Fe		−1.48		
114	Me	Me	$L^1 = PPh_3$	CH$_3$CN	−1.79	+0.35	[34]
115			$L^2 = IMes_2$		−2.01	+0.05	
116	Et	Et	$L^1 = IMe_2$		−2.02	+0.16	
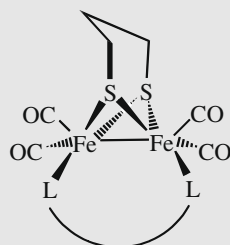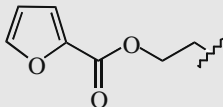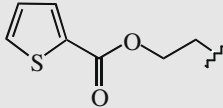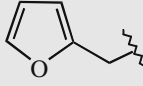
Solvent: acetonitrile

Compounds	L–L	E_{pc}	E_{pa}	Reference
117	Ph$_2$PCH$_2$PPh$_2$	−2.28		51
118	Ph$_2$PN(n-Pr)PPH$_2$	−2.25	+0.33	28
119	Ph$_2$PCH$_2$CH$_2$PPh$_2$	−2.23	+0.07	44

Table 3.1 (*continued*)

Compounds	R	All CO ligands except	Solvent	E_{pc}	E_{pa}	Reference
120	H		CH$_3$CN	−1.58	+0.59	[52]
121		L^1 = PPh$_3$		−1.70	+0.51	
122		L^1 = PMe$_3$		−1.88	+0.19	
123	*n*-Pr	L^2 = PTA	CH$_3$CN	−1.909		[41]
124		L^1 = L^5 = PTA		−2.128		
125		L^2 = DAPTA		−1.784		
126		L^1 = Re-ligand	CH$_3$CN	−1.66	+0.37	[53]
127		L^3, L^6 = Ph$_2$PCH$_2$PPh$_2$	CH$_3$CN	−2.25		[51]
128	*i*-Pr		CH$_3$CN	−1.62 ($E°_1$)[n]		[31]
129		L^2, L^2 = 1,10-phenanthroline	CH$_3$CN	∼−2.2		[54]
130		L^1, L^2 = Ph$_2$PCH$_2$CH$_2$PPh$_2$	CH$_3$CN	−2.01	−0.30	[44]
131		**130** protonated at N	CH$_3$CN	−1.53		[54]
132		L^3, L^6 = Ph$_2$PCH$_2$CH$_2$PPh$_2$	CH$_3$CN	−2.12	+0.08	[44]
133	*t*-Bu		CH$_3$CN	−1.69	+0.67	[55]
134		L^1 = Fe-ligand		−1.50	+0.27	
135	*c*-C$_5$H$_9$		CH$_3$CN	−1.663	+0.547	[56]
136	*c*-C$_6$H$_{11}$			−1.656	+0.588	
137	*c*-C$_7$H$_{13}$			−1.685	+0.575	
138	*c*-C$_5$H$_9$	L^1 = L^6 = PMe$_3$		−1.997	−0.212	
139	*c*-C$_6$H$_{11}$	L^2 = L^6 = PMe$_3$		−1.993	−0.205	
140	*c*-C$_7$H$_{13}$	L^2 = L^6 = PMe$_3$		−1.999	−0.221	
141	CH$_3$OCH$_2$CH$_2$		CH$_3$CN	−1.60 ($E°_1$)[o]		[31]
142		**141** protonated on N	CH$_3$CN	∼−1.2		[57]
143		L^1, L^2 = Ph$_2$PCH$_2$CH$_2$PPh$_2$	CH$_3$CN	−1.98	−0.26	[44]
144		L^3, L^6 = Ph$_2$PCH$_2$CH$_2$PPh$_2$		−2.10	+0.08	
145	BrCH$_2$CH$_2$		CH$_3$CN	−1.63	+0.59	[58]
146	CH$_3$C(O)SCH$_2$CH$_2$			−1.62	+0.56	
147				−1.63	+0.53	
148				−1.64	+0.56	
149	4-MeC$_6$H$_4$SO$_2$NHCH$_2$CH$_2$		CH$_3$CN	−1.63	+0.50	[59]
150	C$_6$H$_5$CH$_2$		CH$_3$CN	−1.57		[60]
151		L^1 = P(pyrr)$_3$		−1.60		
152		L^1 = L^4 = P(pyrr)$_3$		−1.63		
153		L^1 = L^5 = PMe$_3$	CH$_3$CN	−2.18[p]	−0.26[p]	[61,62]
154		**153** protonated at N		−1.55[p]	+0.01[p]	
155		**153** protonated at Fe−Fe		−1.10[p]	+0.65[p]	
156		Doubly protonated **153**; at N and Fe−Fe		−1.00[p]	+1.38[p]	
157	2-BrC$_6$H$_4$CH$_2$		CH$_3$CN	−1.56	+0.61	[63]
158		**157** protonated at N		−1.09		
159	2-FC$_6$H$_4$CH$_2$			−1.56	+0.67	
160	3-BrC$_6$H$_4$CH$_2$			−1.56	+0.67	
161	2-BrC$_6$H$_4$CH$_2$	L^1 = L^4 = PMe$_3$		−2.18	−0.13	
162		**161** protonated at N		−1.49		
163	4-BrC$_6$H$_4$CH$_2$		CH$_3$CN	−1.56		[64]
164	**163** protonated at N			∼−1.16		
165			CH$_3$CN	−1.55	+0.73	[65]
166	**165** protonated at N			−1.13		

Table 3.1 (continued)
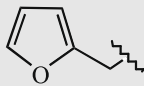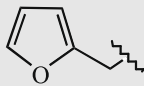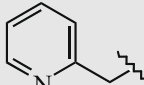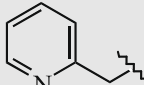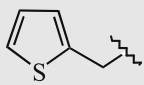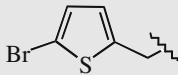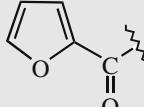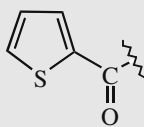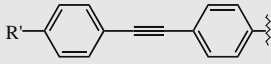
Compounds	R	All CO ligands except	Solvent	E_{pc}	E_{pa}	Reference
167			CH_3CN	−1.55		[66]
168		$L^1 = L^5 = IMe_2$		−2.53	−0.22	
169				−1.54		
170		$L^1 = L^5 = IMe_2$		−2.49	−0.30	
171			CH_3CN	−1.64	+0.65	[67]
172				−1.54	+0.72	
173	$MeC(O)SCH_2C(O)$		CH_3CN	−1.49	+0.86	[68]
174	$EtOC(O)CH_2C(O)$			−1.51	+0.87	
175				−1.54	+0.81	
176				−1.52	+0.82	
177	$4\text{-}CH_3C_6H_4$		CH_3CN	−1.55	+0.55	[69]
178		$L^3 = L^6 = 4\text{-}IC_6H_4NC$		−1.70	+0.13	
179	$4\text{-}CF_3C_6F_4$		CH_3CN	−1.53	+0.89	[70]
180	$4\text{-}CF_3C_6H_4$			−1.54	+0.61	
181	$4\text{-}CF_3C_6F_4$	$L^1 = PPh_3$		−1.74	+0.44	
182	$4\text{-}CF_3C_6H_4$	$L^1 = PPh_3$		−1.73	+0.41	
183	$4\text{-}BrC_6H_4$		CH_3CN	−1.53	+0.54	[71]
184	$4\text{-}IC_6H_4$			−1.54	+0.56	
185	$4\text{-}BrC_6H_4$	$L^1 = PPh_3$	CH_2Cl_2	−1.90	+0.34	
186	$4\text{-}Me_3SiC{\equiv}C$		CH_3CN	−1.55	+0.64	
187	$4\text{-}NO_2C_6H_4$		CH_3CN	−1.39 $(E^{\circ}{}_1)^q$	+0.70	[72]
188	$4\text{-}NH_2C_6H_4$			−1.56	+0.16^r	
189	$4\text{-}MeOC_6H_4$		CH_3CN	−1.61	+0.48	[73]
190	$4\text{-}MeOC_6H_4$	$L^1 = PPh_2H$		−1.78	+0.26	
191	$4\text{-}MeOC(O)C_6H_4$		CH_3CN	−1.54	+0.55	[74]
192	$4\text{-}MeOC(O)C_6H_4$	$L^1 = PPh_3$	CH_3CN	−1.67	+0.34	[75]
193	$4\text{-}MeOC(O)CH_2C_6H_4$		CH_3CN	−1.57		[76]
	R for **194-203**		CH_3CN			[77]
194	$R' = NO_2$			−1.56	+0.55	
195	$R' = CHO$			−1.56	+0.61	
196	$R' = NH_2$			−1.58	+0.46^s	
197	$R' = COOH$			−1.59	+0.64	
198	$R' = COOEt$			−1.56	+0.60	
199	$R' = F$			−1.56	+0.57	
200	$R' = H$			−1.54	+0.55	
201	$R' = CH_3O$			−1.56	+0.55	
202	$R' = NMe_2$			−1.55	+0.50^t	
203	$R' = NO_2$	$L^1 = PPh_3$		−1.67	+0.52	
204	$4\text{-}IC_6H_4$	$L^1 = PPh_3$		−1.67	+0.44	
205	Ru-ligand 2		CH_3CN	−1.49	+0.65	[71]
206	Ru-ligand 3		CH_3CN	−1.49		[78]

Table 3.1 (*continued*)

Compounds	X	Solvent	E_{pc}	E_{pa}	Reference
207	O	CH$_3$CN	−1.59	+0.81	[79]
208	S	CH$_3$CN	−1.48 ($E°_{ov}$)[u]		[80]
		CH$_3$CN	−1.448 ($E°_{ov}$)[v]		[81]

Compounds	All R = H except	All L = CO except	Solvent	($E°_{ov}$)	($E°_1$)	($E°_2$)	Reference
209			CH$_3$CN	−1.27			[82]
			CH$_2$Cl$_2$	−1.44			[20]
			CH$_3$CN	−1.32	−1.33	−1.31	[83]
			CH$_3$CN	−1.31			[84]
210	R^2 = Me			−1.33			
211	R^1 = Cl			−1.20			
212		L^1 = P(OMe)$_3$	CH$_3$CN	−1.48			[82]
213		L^1 = L^2 = PMe$_3$	CH$_3$CN	−2.09 (E_{pc})			[84]
214	R^2 = Me			−2.08 (E_{pc})			
215	R^1 = Cl			−1.91 (E_{pc})			
216	**215** protonated at Fe–Fe			−1.07			
217	R^1 = OH		CH$_3$CN	−0.586			[85]
				−1.24[w]			
218	R^1 = OH	L^1 = PPh$_3$		−0.726			
				−1.54[w]			
219	R^1 = OH	L^1 = L^2 = PPh$_3$		−0.886			
				−1.64[w]			
220	R^1 = OH		CH$_3$CN	−1.279	−1.400	−1.158	[86]
221	R^1 = OH, R^2 = MeO			−1.315	−1.460	−1.170	
222	R^1 = OH, R^2 = Me			−1.283	−1.407	−1.159	
223	R^1 = OH, R^2 = t-Bu			−1.274	−1.403	−1.146	
224	R^1 = OH, R^2 = Cl			−1.222	−1.326	−1.119	
225	R^1 = OH, R^2 = Br			−1.219	−1.298	−1.140	
226	R^1 = MeO			−1.342	−1.389	−1.296	

Other complexes

Compounds	Structure	Solvent	E_{pc}	E_{pa}	Reference
227	[Fe$_2$(SRS)(CO$_6$)]; R is the carborane, 1,2-*closo*-C$_2$B$_{10}$H$_{10}$	CH$_3$CN	−0.88 ($E°_1$)[x]		[87]
228	[Fe$_2$(SRS)(CO$_6$)]; R = CH$_2$C(O)CH$_2$	CH$_3$CN	−1.52	+1.01	[33]
229		CH$_3$CN	−1.28		[88]

$$[Fe_2 (SRS)(CO)_5 L]$$

L = CO; X = CH;   R =

| **230** | L = CO; X = N | | −1.18 | | |
| **231** | L = PPh$_3$, X = CH[i] | | −1.47 | | |

Table 3.1 (continued)
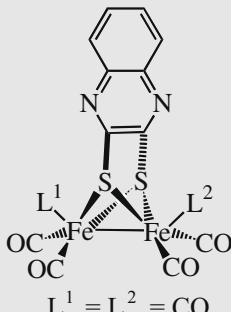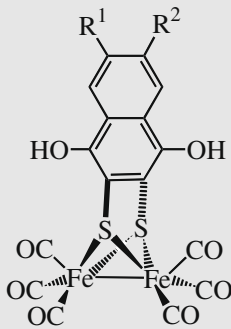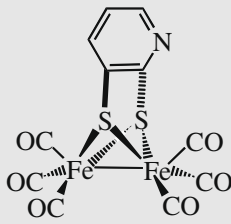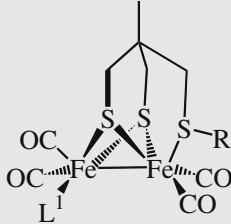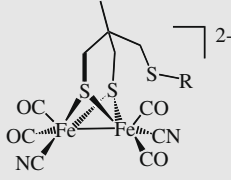
Compounds	Structure	Solvent	E_{pc}	E_{pa}	Reference
232		CH$_3$CN	−1.18 (E°_{ov}) (2-electron process)		[84]
	L^1 = L^2 = CO				
233	L^1 = L^2 = PMe$_3$		−1.88 (E°_{ov}) (2-electron process)		
234		CH$_2$Cl$_2$	−1.341 (E°_{ov}) (2-electron process)		[86]
235	R^1, R^2 = CH=CH−CH=CH		−1.38 (E°_{ov}) (2-electron process)		
236		CH$_3$CN	−1.237 (E°_{ov}) (2-electron process)		
237	L^1 = CO; R = Me	CH$_3$CN	−1.77	+0.28	[25]
238	L^1 = CO; R = C$_6$H$_5$CH$_2$		−1.75	+0.38	
239	L^1 = CN$^−$; R = Me		−2.22	−0.22	
240	L^1 = CN$^−$; R = C$_6$H$_5$CH$_2$		−2.22	−0.27	

Table 3.1 (*continued*)

Compounds	Structure	Solvent	E_{pc}	E_{pa}	Reference
241	R = Me (position of cyanide ligands not reported	$\leqslant -2.8$	-0.64		
242	R = $C_6H_5CH_2$ (position of cyanide ligands not reported	$\leqslant -2.8$	-0.65		
243	$[Fe_2(SCH_2CH(OR)CH_2S)(CO_6)]$; R = tetra-*O*-acetyl-β-D-glucopyranoside	CH_3CN	-1.64	$+0.95$	[98]
244	$[Fe_2(SCH_2CH(OR)CH_2S)(CO_6)]$; R = β-D-glucopyranoside		~ -1.64		

^a For structures of special substituents and ligands see Table 3.2. Potentials (V) vs. the standard potential of the Fc^+/Fc couple in acetonitrile, unless otherwise indicated. Data are reported for N_2 or Ar purge except as noted.

^b PC = propylene carbonate.

^c Without CO. Potentials are 60–90 mV more negative under a CO atmosphere.

^d Referred to ferrocene in CH_2Cl_2.

^e -1.59 V under CO.

^f Without CO. $E° = -0.632$ V under a CO atmosphere.

^g Standard potential for the first one-electron reduction; $E°_2 = -1.80$ V.

^h Under CO atmosphere.

ⁱ Potentials vs. ferrocene in CH_2Cl_2.

^j Isomeric identity uncertain.

^k Isomeric identity uncertain.

^l Standard potential for the first one-electron reduction; $E°_2 = -1.47$ V.

^m Standard potential for the first one-electron reduction; $E°_2 = -1.42$ V.

ⁿ Standard potential for the first one-electron reduction; $E°_2 = -1.63$ V.

^o Standard potential for the first one-electron reduction; $E°_2 = -1.60$ V.

^p Peak potentials from differential pulse voltammetry.

^q Standard potential for the first one-electron reduction; $E°_2 = -1.75$ V. These reductions may be centered on the nitrophenyl group.

^r Possibly associated with the oxidation of the 1,4-diaminobenzene group in the bridging ligand.

^s Anodic peak at +0.23 V for oxidation of aniline function precedes this peak.

^t Anodic peak at +0.20 V for oxidation of dimethylaminophenyl group precedes this peak.

^u An overall two-electron reduction with inverted potentials. $E°_{ov} = (E°_1 + E°_2)/2$ where $E°_1$ and $E°_2$ are the standard potentials for insertion of the first and second electrons, respectively. Value of $E°_{ov}$ estimated from Fig. 4 of Ref. [80].

^v See footnote u. $E°_1$ and $E°_2$ estimated to be -1.505 and -1.390 V, respectively.

^w 1.5 equiv. of Bu_4NOH added. Potentials correspond to two "redox waves" associated with the quinone/quinone anion radical and quinone anion radical/quinone dianion processes.

^x $E°_2 = -1.13$V.

3. Tabulated data

3.1. Tabulated reduction and oxidation peak potentials

Table 3.1 summarizes all of the collected data including compound structures and peak potentials. While the structural drawings clearly depict substituents, they are misleading with regard to the three-dimensional structure of the complexes. For example, the axis through the two sulfur atoms and that through the two iron atoms in the Fe_2S_2 core are perpendicular. Consequently, a more accurate depiction is shown below for compound **209**.

This compound contains three bridges: two sulfur atoms that bridge the two iron atoms and the C_6H_4 group that connects the two sulfurs. In this review, the terms "bridge", "bridged", "bridging group" or "bridging ligand" will refer to the dithiolato group or ligand in complexes with a μ-(SXS)Fe_2S_2 core.
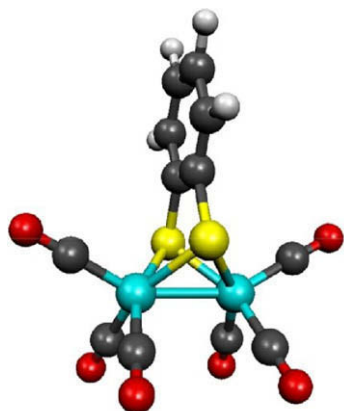
Structures of unusual ligands and substituent groups are presented in Table 3.2.

4. Discussion

4.1. Reduction potentials

### 4.1.1. Effect of the bridging or nonbridging group with all carbon atoms

For purposes of comparison, it is convenient to restrict the discussion in this section to cases where all of the remaining ligands at Fe_2 are CO. For example, we may compare an unbridged complex containing alkyl substituents, **7**, whose E_{pc} is -1.71 V with an example of a 1,2-ethanedithiolato bridge, **34**, -1.67 V and further with the 1,3-propanedithiolato bridge, **36**, for which an average value of -1.66 ± 0.06 V has been reported. For **34** and **36**, the values obtained from the same laboratory are -1.67 and -1.71 V, respectively. Nevertheless, the scatter in the experimental results exhibited by **36** leaves it uncertain whether there is any effect of the nature of the alkyl substituents, either bridged or unbridged. The 1,2-xylenediyl group (resembling two benzyl groups) at -1.56 V **20** may be statistically more easily reduced. On the other hand, the unbridged complex with two phenyl substituents **15** falls at -1.44 V, which is definitely lower than those with alkyl groups. There is also an appreciable effect of substituents on the phenyl groups **16–18** wherein the potential is more negative for the electron-donating 2- and 4-MeO groups and less negative for the electron-withdrawing Cl substituent. In all cases, comparisons have been and will be made for compounds studied in the same solvent, CH_3CN.

### 4.1.2. Effect of X in SCH_2XCH_2S bridges

There are four examples for μ-SCH_2XCH_2S complexes with X = CH_2 (**36**), X = NH (**120**), X = O (**207**) and X = S (**208**). The values of E_{pc} are -1.66 ± 0.06 V, -1.58 V, -1.59 V and -1.48 or -1.45 V, respectively, with the values for X = S being $E°_{ov}$ for the overall two-electron reversible reduction. The trend for ease of reduction is S > O ~ NH > CH_2. However, it is not clear that O, NH and CH_2 are significantly different whereas S is definitely more easily
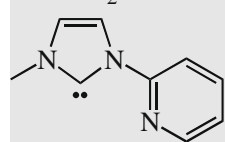
Table 3.2
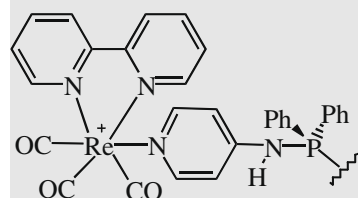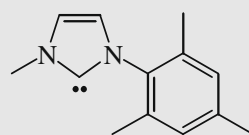Table of ligands and substituent groups.

Phosphines

P(pyd)₃ =

P(pyrr)₃ =

PTA =

DAPTA =

Carbenes
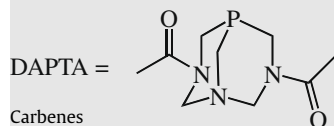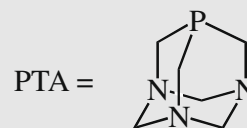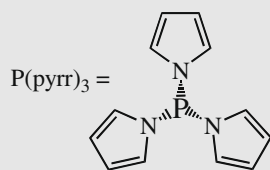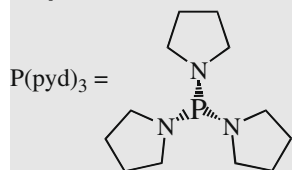
IMe₂

IMesMe
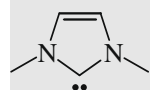
IMes₂

IPyMe

IPic₂

CH₂(IMe)₂

Substituent groups

Re-ligand
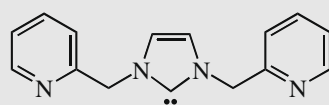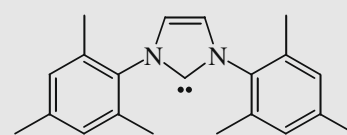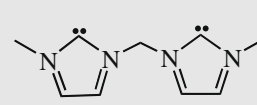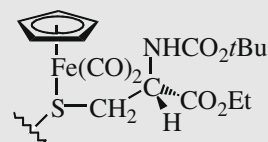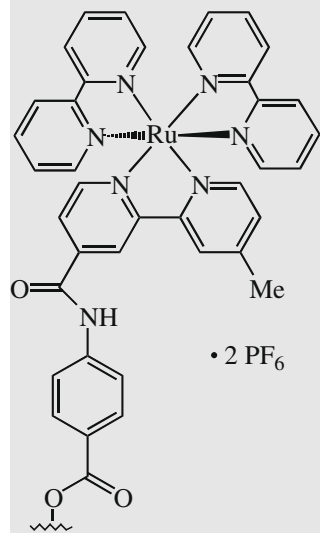
Fe-ligand

Ru-ligand 1
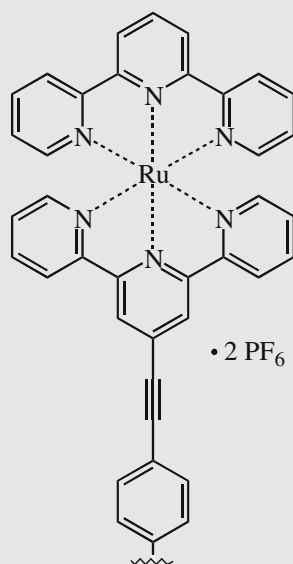
Ru-ligand 2
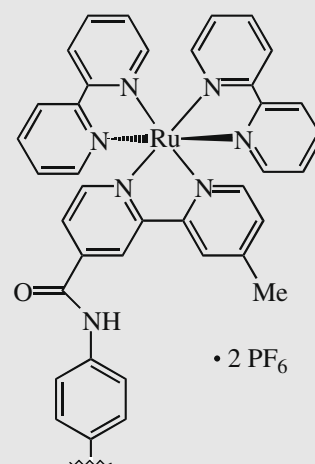
Ru-ligand 3

Table 4.1
Effect of replacing CO by phosphine or phosphite in μ-S(CH$_2$)$_3$S complexes.[a]

Compounds	Phosphine or phosphite (L)	E_{pc} (V) (One L)[b]	E_{pc} (V) (Two L)[b]	ΔE_{pc} (V) (One L)	ΔE_{pc}/2 (V) (Two L)
47, **58**	PMe$_3$	−1.94	−2.31 ± 0.05	−0.28	−0.32
48, **54**	PMe$_2$Ph	−1.90	−2.30	−0.24	−0.20
49	PPh$_3$	−1.84		−0.18	
50, **55**	P(OEt)$_3$	−1.81	−2.27	−0.15	−0.30
56, **57**	P(OMe)$_3$	−1.98	−2.30	−0.32	−0.32
74, **75**	PTA	−1.94	−2.14 ± 0.06	−0.28	−0.24
78, **79**	DAPTA	−1.83	−2.06	−0.17	−0.20
81	P(pyd)$_3$	−1.98		−0.32	

[a] Acetonitrile as solvent. Potentials are vs. ferrocene in acetonitrile. Data taken from Table 3.1. $\Delta E_{pc} = E_{pc}$(one or two L replacing CO) − E_{pc}(all CO), where E_{pc}(all CO) = −1.66 V. See Table 3.2 for structures of PTA, DAPTA and P(pyd)$_3$.
[b] One L: One L replacing a CO; Two L: One L replacing CO on each of the iron atoms.

reduced. Nevertheless, the effect is quite small, of the order of 0.1 V (2 kcal/mol).

4.1.3. Effect of R in SCH$_2$CH(R)CH$_2$S bridges

Five compounds **37**, **39**, **42**, **44**, **45** with alkyl, carboxylic acid, or amide substituents have E_{pc}-values falling in the range of −1.61 to −1.67 V, quite similar to the unsubstituted complex **36**, −1.66 ± 0.06 V. However, esterified OH **40**, **41** at −1.58 and −1.59 V may be reduced at a lower potential. Nevertheless, R substituents have little effect on the reduction potential in SCH$_2$CH(R)CH$_2$S bridged complexes.

4.1.4. Effect of R in SCH$_2$N(R)CH$_2$S bridges

There are more than forty examples of complexes of the type [(μ-SCH$_2$NRCH$_2$S)Fe$_2$(CO)$_6$] and the values of E_{pc} of these complexes fall in the narrow range of −1.5 to −1.7 V with no clear correlation with the nature of R. The average value of E_{pc} for these complexes is −1.56 V with a standard deviation of 0.02 V. Just as with substitution at carbon two in complexes with 1,3-propanedithiolato bridges, E_{pc} for [(μ-SCH$_2$NRCH$_2$S)Fe$_2$(CO)$_6$] is virtually independent of R. This is understandable in both cases as the substituents are well insulated from the diiron core where the LUMO is concentrated.

4.1.5. μ-Arenedithiolato bridges

As mentioned above there is a significant increase in the ease of reduction on going from the propanedithiolato complex **36** (E_{pc} = −1.66 V) to the complex with two benzenethiolato ligands, **15** (E_{pc} = −1.44 V). This trend continues with the 1,2-benzenedithiolato complex **209** which is even more easily reduced ($E°_{ov}$ = −1.30 ± 0.04 V). Interestingly, the 1,2-benzenedithiolato complex undergoes a reversible, two-electron reduction with an overall standard potential, $E°_{ov}$, in contrast to the propanedithiolato complex **36** whose first stage of reduction is a one-electron reaction. All reported complexes with an arenedithiolato bridge appear to exhibit a reversible two-electron reduction. In particular for **209**, the mechanism of the reduction and the structural changes associated with it have been discussed in detail [83].

Substitution on the benzene ring causes small changes in $E°_{ov}$ that are consistent with the electron-donating or withdrawing nature of the substituents **210**, **211**, **220–226**. Included in the series are various hydroquinone-type complexes **220–225**, **234**, **235** all of which exhibit the reversible two-electron reduction process. 2,3-Quinoxalinedithiolato complex **232** and the complex derived from 2,3-pyridinedithiol (**236**) are more easily reduced than the carbocyclic arene complexes in keeping with the greater electronegativity of nitrogen compared to carbon.

4.1.6. Effect of replacing CO by phosphine or phosphite

Contrary to the rather minor effects of structural changes in the bridging ligand, changing the carbonyl ligands on the iron centers can have a substantial effect on reduction and oxidation potential. Table 4.1 shows the effects in the case of a 1,3-propanedithiolato bridge.

The data indicate that replacing CO with phosphine causes a 0.2–0.3 V decrease in the ease of reduction of the complexes and, for those cases where data are available, and with one exception, replacement of a second CO by phosphine causes nearly an identical additional shift reflecting the additivity of the effect. The results for the two phosphites are anomalous in that one shows a smaller shift than seen with the phosphines and the other a larger shift.

The effect of replacing CO by phosphine can be explained by the fact that the two ligands are both good σ donors but CO undergoes significantly greater π backbonding than the phosphines included in Table 4.1 [91]. The very large shift caused by tris(N-pyrrolidinyl)phosphine, P(pyd)$_3$, is consistent with its being a better donor ligand than PMe$_3$ [43]. There is no clear indication of whether a basal or an apical phosphine is more effective in decreasing the electron affinity of the complex. Though X-ray crystallographic structures are often available, it is known that isomerization occurs in solution so the electrochemistry is sampling a mixture of isomers that are probably rapidly interconverting [44,92–94]. Another recent example involves phosphite complexes **56** and **57** [37].

Replacement of two CO ligands by the bidentate ligand, Ph$_2$PCH$_2$CH$_2$PPh$_2$ (apical, basal on one Fe) (**86**), has very nearly the same effect as using two PMePh$_2$ monophosphine ligands, one on each Fe (**54**). The cathodic peak potential for the chelating diphosphine is −2.33 V while that for complex with two PMePh$_2$ ligands is −2.30 V. Similarly, diphosphines connecting the two iron atoms (cis basal, basal), compounds **117–119**, are reduced in this same region, E_{pc} = −2.28, −2.25 and −2.23, respectively. Two dissimilar monophosphines or phosphites also produce cathodic peak potentials in this region (compounds **63–69**, **80**), −2.06 to −2.23 V.

Turning to the [(μ-SCH$_2$NRCH$_2$S)Fe$_2$(CO)$_6$] system, similar effects of substituting a phosphine for one or two CO ligands have been seen. Some results are summarized in Table 4.2. As pointed out above, the identity of R has little influence on the potentials so with some confidence we can attribute the effects of the phosphine ligands solely to the phosphine with no contribution from R. With this in mind, one sees substantial negative shifts in reduction potential for PMe$_3$, a strong donor ligand (with the exception of R = cycloalkyl where the shift is unaccountably smaller). PPh$_3$ is generally a weaker donor ligand and the potential shifts are smaller than for PMe$_3$. PTA is a very strong donor but its acetylated derivative, DAPTA, is weaker due to the electron-withdrawing acetyl groups. Finally, it should be noted that tris(N-pyrrolyl)phosphine, P(pyrr)$_3$, causes a tiny shift, 30 mV per phosphine ligand, reflecting the fact that it is an exceptionally weak donor ligand [60].

Table 4.2
Effect of replacing CO by phosphine on reduction potentials of $(\mu\text{-SCH}_2\text{NRCH}_2\text{S})\text{Fe}_2(\text{CO})_6$.[a]

Compounds	R	Phosphine (L)	E_{pc} (all CO)	E_{pc} (one L replacing CO)	E_{pc} (two L replacing CO)	ΔE_{pc} (One L)	$\Delta E_{pc}/2$ (Two L)
120, 122	H	PMe$_3$	−1.58	−1.88		−0.30	
157, 161	2-BrC$_6$H$_4$CH$_2$		−1.48		−2.10		−0.31
135, 138	c-C$_5$H$_9$		−1.663		−1.997		−0.167
136, 139	c-C$_6$H$_{11}$		−1.656		−1.993		−0.168
137, 140	c-C$_7$H$_{13}$		−1.685		−1.999		−0.157
120, 121	H	PPh$_3$	−1.58	−1.70		−0.12	
179, 181	4-CF$_3$C$_6$F$_4$		−1.53	−1.74		−0.21	
180, 182	4-CF$_3$C$_6$H$_4$		−1.54	−1.73		−0.19	
123, 124, 128	n-Pr	PTA	−1.62[b]	−1.909	−2.128	−0.29	−0.25
128, 125	n-Pr	DAPTA	−1.62[b]	−1.784		−0.16	
150–152	C$_6$H$_5$CH$_2$	P(pyrr)$_3$	−1.57	−1.60	−1.63	−0.03	−0.03

[a] All potentials in V vs. ferrocene in acetonitrile.
[b] Estimated. Set equal to R = i-Pr (**128**).

4.1.7. Heterocyclic carbene complexes

These complexes are based on N,N′-substituted imidazol-2-yli-dene, ligands which are strong donors similar to phosphines. Like phosphines, heterocyclic carbene ligands cause a shift in reduction potential to more negative values. For example, for complexes containing the μ-S(CH$_2$)$_3$S bridge, the complexes with an IMes$_2$, IMesMe and IMe$_2$ replacing CO (**103–105**) have E_{pc}-values of −2.10, −2.06 and −2.05 ± 0.05 V, respectively (see Table 3.2 for structures of these carbenes). These should be compared with the all-CO complex **36** whose cathodic peak potential is −1.66 V. The carbene complexes exhibit even larger negative shifts than phosphine complexes, E_{pc} being −1.94 for the PMe$_3$ complex **47**, attesting to the strong donor properties of the carbenes.

As with the phosphine complexes, a second carbene ligand causes an additional shift almost equal to that seen with the first carbene. This is illustrated by $(\mu\text{-S(CH}_2)_3\text{S})\text{Fe}_2(\text{CO})_6$ (**36**), $(\mu\text{-S(CH}_2)_3\text{S})[\text{Fe(CO)}_3][\text{Fe(CO)}_2\text{IMe}_2]$ (**105**) and $(\mu\text{-S(CH}_2)_3\text{S})\text{-}[\text{Fe(CO)}_2\text{IMe}_2]_2$ (**109**) whose cathodic peak potentials are −1.66, −2.05 and −2.52 ± 0.06 V, respectively. This corresponds to a −0.39 V shift with one carbene and an average shift per carbene of −0.43 V for the bis-carbene complex. As can be seen by comparison with results shown in Table 4.1, these shifts are even larger than seen with phosphines.

4.1.8. Other ligands

n-Propylamine brings about a small negative shift in reduction potential, E_{pc} = −1.80 V in the complex containing the μ-S(CH$_2$)$_3$S bridge **87**. This can be compared with the all-CO complex, **36**, at −1.66 V. Sulfide ligands cause a barely significant negative shift **89–91** whereas sulfoxides **92, 93** had no effect. Methyl isocyanide caused a moderate shift to −1.81 V for the first ligand (−0.15 V shift) and an additional −0.27 V shift for the second **94, 95**. Cyanide **96, 100** causes a very large shift, −0.51 V for the first cyanide and an additional −0.55 V for the second.

By contrast, large positive shifts in reduction potential have been reported for the very strong acceptor ligand, NO$^+$ **101, 102** (**28** and **29** for complexes with a 1,2-ethanedithiolato bridge). Though a quantitative measure of the shift on replacing CO by NO$^+$ is not possible, it must be larger than one volt.

4.1.9. Effect of protonation of the complexes

Some complexes are sufficiently basic to be protonated by moderately strong acids, either when a ligand contains a basic site or protonation of the Fe–Fe bond can occur, as when some phosphine or heterocyclic carbene ligands are present. It is uniformly found that protonated complexes are more readily reduced than the unprotonated form. Table 4.3 shows a number of examples. This table is an augmented version of Table 1 from Ref. [95].

The differences in reduction potentials for protonated and unprotonated forms are of two types: complexes where protonation occurs at the iron–iron bond and those where a ligand is protonated, all at a nitrogen atom. For the former, the differences are large, ranging from +0.75 to +1.08 and for the latter much smaller differences accrue, +0.38 to +0.69. These differences have been rationalized in terms of the differing basicities of the unreduced complex and the species formed on one-electron reduction [95]. Application of a thermodynamic cycle shows that $E°(\text{M–H}^+) − E°(\text{M}) = (2.303RT/F)(pK_a(\text{M–H}) − pK_a(\text{M–H}^+))$ where $E°(\text{M H}^+)$ and $E°(\text{M})$ are the standard potentials for reduction of the protonated and unprotonated complexes, respectively, and $pK_a(\text{M–H})$ and $pK_a(\text{M–H}^+)$ correspond to the protonated reduced and oxidized forms, respectively. Consequently, the standard potential for reduction of the protonated form compared to the unprotonated form will reflect the increase in basicity of the reduced form compared to the oxidized form. As the reduced forms of these complexes have substantial increases in electron density at the Fe–Fe bond, protonation there corresponds to a very large value of $pK_a(\text{M–H})$ and a large positive shift in $E°(\text{M–H}^+)$. On the other hand, protonation on a ligand occurs at sites where the increase in electron density upon reduction is more muted leading to smaller $pK_a(\text{M–H})$ and hence less positive $E°(\text{M–H}^+)$. Though the potentials reported in Table 4.3 are not standard potentials, the trends follow exactly these expectations with protonation on the Fe–Fe bond leading to large shifts in potential and protonation on a ligand giving smaller shifts.

4.2. Oxidation potentials

Examination of the data reveals that the anodic peak potentials are affected by ligand identity in a manner that is completely analogous to the cathodic peak potentials. For purposes of illustration, the discussion will center on complexes with a 1,3-propanedithiolato bridge. Results are summarized in Table 4.4.

Strong donor ligands are expected to facilitate the removal of an electron causing a negative shift in the oxidation potentials. This is readily evident in Table 4.4. Here, the negative shift for replacement of one CO by PMe$_3$, −0.57 V, is almost twice as large as the shift in reduction potential, −0.28 V (Table 4.1). For all ligands for which data are available, the shifts in oxidation potential are much larger than shifts in reduction potential. This greater sensitivity to changes in ligand donor strength for oxidation as compared to reduction may be attributed to the HOMO being concentrated on Fe–Fe so that good donor ligands attached to Fe will make it much easier to remove an electron. However, reduction involves the LUMO, which is less metal-centered with Fe–S contributions making the reductions less sensitive to strong donor ligands.

Table 4.3
Reduction potentials of unprotonated (E_{pc}(M)) and protonated (E_{pc}(M–H$^+$)) complexes in acetonitrile. Potentials are in V vs. ferrocene in acetonitrile. (This is an augmented version of Table 1 from Capon et al. [95]. Some numerical entries are different due to different choices of reference electrode potentials).

Compounds	No.	E_{pc} (M)	Protonation site	E_{pc}(M–H$^+$)	$\Delta E_{pc} = E_{pc}$(M–H$^+$) − E_{pc}(M)	Reference
[Fe$_2$(μ-adt)(CO)$_6$][a]	**141**	−1.60	N	∼−1.2	∼0.4	[57]
[Fe$_2$(μ-pdt)(CO)$_4$(PMe$_3$)(CN)$^-$] [b]	**97**	−2.58	Fe–Fe	−1.57	1.01	[38,46]
			Fe–Fe and CN$^-$	−1.42		
[Fe$_2$(μ-pdt)(CO)$_4$(PMe$_3$)$_2$] [b]	**58**	−2.31	Fe–Fe	−1.39	0.92	[38]
		−2.25		−1.50	0.75	[7]
[Fe$_2$(μ-pdt)(CO)$_4$(PTA)$_2$][b,c]	**75**	−2.18	PTA (2X)	−1.75	0.43	[7]
[Fe$_2$(μ-bdt)(CO)$_4$(PMe$_3$)$_2$][d]	**215**	−1.91	Fe–Fe	−1.07	0.84	[84]
[Fe$_2$(μ-adt)(CO)$_4$(PMe$_3$)$_2$][e]	**153**	−2.18	Fe–Fe	−1.10	1.08	[61,62]
			N	−1.55	0.63	
			N and Fe–Fe	−1.00		
[Fe$_2$(μ-adt)(CO)$_6$][f]	**163**	−1.56	N	−1.18	0.38	[64]
[Fe$_2$(μ-adt)(CO)$_6$][g]	**157**	−1.56	N	−1.09	0.47	[63]
[Fe$_2$(μ-adt)(CO)$_4$(PMe$_3$)$_2$][g]	**161**	−2.18	N	−1.49	0.69	
[Fe$_2$(μ-adt)(CO)$_6$][h]	**165**	−1.55	N	−1.13	0.42	[65]
[Fe$_2$(μ-adt)(CO)$_4$(κ^2-dppe)][i]	**130**	−2.01	N	−1.53	0.48	[44,57]
[Fe$_2$(μ-pdt)(CO)$_4$(κ^2-CH$_2$(IMe)$_2$)] [b,j]	**112**	−2.42	Fe–Fe	−1.48	0.94	[50]
[Fe$_2$(μ-pdt)(CO)$_4$(κ^2-(Ph$_2$PCH$_2$)$_2$NMe)]	**110**	−2.3	Fe–Fe[k]	−1.26	1.0	[39]
	110	−2.3	N[l]	−1.9	0.4	

[a] adt = (SCH$_2$)$_2$N(CH$_2$CH$_2$OMe).
[b] pdt = S(CH$_2$)$_3$S.
[c] PTA = 1,3,5-triaza-7-phosphaadamantane.
[d] bdt = 1,2-benzenedithiolato.
[e] adt = (SCH$_2$)$_2$N(CH$_2$C$_6$H$_5$).
[f] adt = (SCH$_2$)$_2$N(CH$_2$C$_6$H$_4$-4-Br).
[g] adt = (SCH$_2$)$_2$N(CH$_2$C$_6$H$_4$-2-Br).
[h] adt = (SCH$_2$)$_2$N(2-furylmethyl).
[i] adt = (SCH$_2$)$_2$N-i-Pr, dppe = 1,2-bis(diphenylphosphino)ethane.
[j] CH$_2$(IMe)$_2$ = I$_{Me}$–CH$_2$–I$_{Me}$, where I$_{Me}$ = 1-methylimidazol-2-ylidene.
[k] Dichloromethane.
[l] Acetone.

The ordering of the size of the shifts is the same for oxidation and reduction: CN– ∼ heterocyclic carbene > phosphine > CH$_3$NC, reflecting the common origin of the two effects. We will assume that the shifts in potential are measures of the relative ligand donor strength. This ordering from the electrochemical data is qualitatively the same as seen in other measures of ligand donor strength such as effects of the ligands on carbonyl stretching frequencies [91].

For a more quantitative comparison, the shifts in reduction and oxidation potential seen upon replacing a CO by various ligands were correlated with Crabtree's computed electronic parameter corrected for vibrational coupling, CEP* [96]. This parameter was evaluated by comparing computations and experimental determination of the A$_1$ v(CO) vibrational frequency in LNi(CO)$_3$ as well as by correlation with other measures of ligand donor strength.

Fig. 4.1 shows a plot of potential shifts (V) vs. CEP* (cm^{-1}) using data taken from Tables 4.1, 4.2 and 4.4 as well as some extracted from Table 3.1. For the reduction potentials one can see that a rea-

sonably linear relationship is obtained with R^2 = 0.980. The largest negative shift is seen for cyanide with progressively smaller shifts for IMe, PMe$_3$, P(OEt)$_3$, Et$_2$S and CH$_3$CN, the shifts decreasing linearly with increasing CEP*. Finally, the very strong electron-accepting ligand, NO$^+$, shows a large positive shift and it also has the
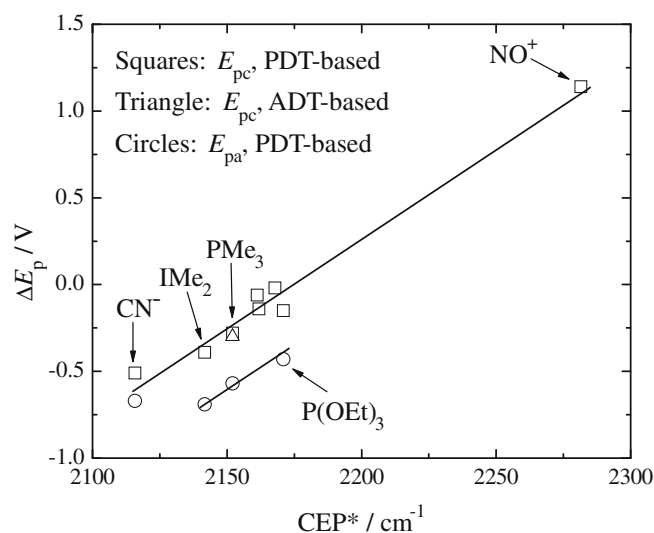
Table 4.4
Anodic peak potentials for complexes containing a 1,3-propanedithiolato bridge.[a]

Compounds	Ligands all CO except	E_{pa} (V) vs. Fc$^+$/Fc	E_{pa} − E_{pa} (all CO) (V)
36		+0.80	–
47	PMe$_3$	+0.23	−0.57
58	PMe$_3$, PMe$_3$	−0.20	−1.00
50	P(OEt)$_3$	+0.37	−0.43
55	P(OEt)$_3$, P(OEt)$_3$	−0.08	−0.88
74	PTA	+0.34	−0.46
75	PTA, PTA	0.00	−0.80
105	IMe$_2$	+0.11	−0.69
109	IMe$_2$, IMe$_2$	−0.24	−1.04
94	CH$_3$NC	+0.63	−0.17
95	CH$_3$NC, CH$_3$NC	+0.21	−0.59
96	CN$^-$	+0.13	−0.67
100	CN$^-$, CN$^-$	−0.39	−1.19

[a] See Table 3.2 for structures of PTA and IMe$_2$.

Fig. 4.1. ΔE_p vs. CEP* for replacement of one CO by the indicated ligands, L. ΔE_p = peak potential for L replacing CO minus peak potential for all-CO reference complex. PDT-based reference is [Fe$_2$(μ-S(CH$_2$)$_3$S)(CO)$_6$] and ADT-based is [Fe$_2$(μ-SCH$_2$NHCH$_2$S)(CO)$_6$]. CEP* is calculated electronic parameter corrected for vibrational coupling from [96]. The three unlabeled ligands are, in order of increasing CEP*, Et$_2$S, n-PrNH$_2$ and MeCN. CEP* for Et$_2$S assumed to equal that of Me$_2$S; n-PrNH$_2$ equal to NH$_3$; P(OEt)$_3$ equal to P(OMe)$_3$. Data for NO$^+$ are for [Fe$_2$(μ-S(CH$_2$)$_3$S)(CO)$_5$(PMe$_3$)] as reference complex and CH$_2$Cl$_2$ as solvent. All other data are for CH$_3$CN. Linear regression equation: ΔE_p = 0.0103CEP* − 22.479 (R^2 = 0.980). Line for three points for E_{pa} is drawn with the same slope as the linear regression. The point for cyanide has been ignored.

Table 4.5
Catalytic reduction of acids.[a]

Compounds	Solvent	Acid	Potential of catalysis (V) vs. Fc[+]/Fc	E°_{HA} (V) vs. Fc[+]/Fc	Overpotential (V)	Catalytic efficiency (C.E.)	Reference
7	CH$_3$CN	Acetic	−2.3	−1.46	−0.8	W (0.05)	[8]
7	THF	Acetic	−2.1			M (0.48)	[15]
8	CH$_3$CN	Acetic	−2.25	−1.46	−0.79	W (0.19)	[8]
10	CH$_3$CN	Acetic	−2.3	−1.46	−0.8	W, dr (0.10)	[17]
14	CH$_3$CN	Acetic	−1.7	−1.46	−0.2	W (0.09)	[18]
15	CH$_3$CN	Acetic	−2.26 (peak at −1.70 V)[b]	−1.46	−0.80	M (0.22)	[19]
19	CH$_3$CN	Acetic	−2.08[b]	−1.46	−0.62		[19]
21	CH$_3$CN	Acetic	−2.2	−1.46	−0.7	S (0.91)	[21]
26	THF	p-Toluene-sulfonic	−1.89			M (0.67)	[15]
36	CH$_3$CN	Acetic	−2.35	−1.46	−0.89	W (0.06)	[7]
36	THF	p-Toluene-sulfonic	−1.73			S, N$_2$ (0.75) W, CO (0.22)	[32]
37	CH$_3$CN	Acetic	−2.5	−1.46	−1.0	M, dr (0.27)	[17]
38	CH$_3$CN	Acetic	−2.3	−1.46	−0.8	M, dr (0.28)	[17]
38	CH$_3$CN	HCl	−1.45	−0.67	−0.78	W, dr? (0.06)	[17]
39	CH$_3$CN	Acetic	−2.4	−1.46	−0.9	W, dr (0.19)	[17]
43	CH$_3$CN (CO)	Acetic	−2.3	−1.46	−0.8	M, dr (0.40)	[34]
51	CH$_3$CN	CF$_3$SO$_3$H	−1.75	−0.29	−1.46	S (1.0), dr	[36]
52	CH$_3$CN	CF$_3$SO$_3$H	−1.7	−0.29	−1.4	S (0.88), dr	[36]
58	CH$_3$CN	p-Toluene-sulfonic	−1.79	−0.65	−1.14	M (0.28)	[38]
58	CH$_3$CN	Acetic	−2.25	−1.46	−0.79	W (0.11)	[7]
59	CH$_3$CN	Acetic	−2.26	−1.46	−0.80	W (0.05)	[7]
71	CH$_3$CN	p-Toluene-sulfonic	−1.7	−0.65	−1.0	M (0.54)	[37]
72	CH$_3$CN	p-Toluene-sulfonic	−1.9	−0.65	−1.2	M (0.30)	[37]
73	CH$_3$CN	HCl	−1.9	−0.67	−1.2	M, dr? (0.28)	[17]
74	CH$_3$CN	Acetic	−1.94	−1.46	−0.48	W (0.03)	[7]
75	CH$_3$CN	Acetic	−2.18	−1.46	−0.72	W (0.08)	[7]
76	CH$_3$CN	Acetic	−2.13	−1.46	−0.67	W (0.10)	[7]
77	CH$_3$CN	Acetic	−1.86[b]	−1.46		W	[7]
80	CH$_3$CN	Acetic	−2.13	−1.46	−0.67	M (0.62)	[42]
81	CH$_3$CN	Acetic	−1.98	−1.46	−0.52	M (0.27)	[43]
93	CH$_3$CN	Acetic	−1.80	−1.46	−0.34	M (0.40)	[27]
97	CH$_3$CN	p-Toluene-sulfonic	−1.1	−0.65	−0.4	M (0.44)	[46]
105	CH$_3$CN	Acetic	−2.10	−1.46	−0.64	M (0.50)	[9]
110	CH$_3$CN	Acetic	−2.1	−1.46	−0.6	W (0.10)	[30]
111	CH$_3$CN	Acetic	−2.3	−1.46	−0.8	S (1.1), dr	[30]
112	CH$_2$Cl$_2$	CF$_3$COOH	−1.6			cnj	[50]
117	CH$_3$CN	CF$_3$SO$_3$H	−2.34	−0.29	−2.05	S (1.0),dr	[51]
118	CH$_3$CN	Acetic	−2.2	−1.46	−0.7	M (0.42)	[28]
125	CH$_3$CN	Acetic	−1.78	−1.46	−0.32	W (0.12)	[41]
125	CH$_3$CN	H$_2$SO$_4$	−1.30	−0.58	−0.72	M (0.62), dr	[41]
126	CH$_3$CN	CF$_3$SO$_3$H	−1.6	−0.29	−1.3	S (0.95)	[53]
130	CH$_3$CN	p-Toluene-sulfonic	−1.53	−0.65	−0.88	M (0.59)	[54]
134	CH$_3$CN	Acetic	−2.15	−1.46	−0.69	M (0.70)	[55]
136	CH$_3$CN	Acetic	−2.1	−1.46	−0.6	cnj	[56]
137	CH$_3$CN	Acetic	−2.2	−1.46	−0.7	cnj	[56]
139	CH$_3$CN	Acetic	−2.15	−1.46	−0.69	cnj	[56]
140	CH$_3$CN	Acetic	−2.1	−1.46	−0.6	cnj	[56]
141	CH$_3$CN	HBF$_4$	−1.3	−0.28	−1.0	M (0.52)	[57]
141	CH$_3$CN	p-Toluene-sulfonic	−1.3	−0.65	−0.6	M (0.29)	[57]
148	CH$_3$CN	Acetic	−2.2	−1.46	−0.7	W (0.22)	[58]
149	CH$_3$CN	CF$_3$SO$_3$H	−1.6	−0.29	−1.3	M (0.74)	[59]
153	CH$_3$CN	HClO$_4$	−1.52	−0.26	−1.26	M (0.40)	[62]
165	CH$_3$CN	HClO$_4$	−1.2	−0.26	−0.9	M (0.32)	[65]
167	CH$_3$CN	HClO$_4$	−1.4	−0.26	−1.1	S (0.85)	[67]
168	CH$_3$CN	CF$_3$COOH	−1.51	−0.89	−0.62	M (0.29)	[66]
170	CH$_3$CN	CF$_3$COOH	−1.72	−0.89	−0.83	M (0.60)	[66]
171	CH$_3$CN	HClO$_4$	−1.45	−0.26	−1.19	M (0.50)	[67]
172	CH$_3$CN	HClO$_4$	−1.25	−0.26	−0.99	M (0.43)	[67]
173	CH$_3$CN	Acetic	−2.2	−1.46	−0.7	M (0.50)	[68]
177	CH$_3$CN	p-Toluene-sulfonic	−1.45	−0.65	−0.80	M (0.40)	[89]
178	CH$_3$CN	p-Toluene-sulfonic	−1.43	−0.65	−0.78	M (0.37)	[69]
179	CH$_3$CN	Acetic	−2.2	−1.46	−0.7	M (0.36), dr	[70]
179	CH$_3$CN	HBF$_4$	−1.5	−0.28	−1.2	M (0.37), dr	[70]
180	CH$_3$CN	Acetic	−2.1	−1.46	−0.6	W (0.23), dr	[70]
180	CH$_3$CN	HBF$_4$	−1.5	−0.28	−1.2	W (0.22), dr	[70]
181	CH$_3$CN	Acetic	−2.2	−1.46	−0.7	M (0.31), dr	[70]
181	CH$_3$CN	HBF$_4$	−1.6	−0.28	−1.3	W (0.18), dr	[70]
182	CH$_3$CN	Acetic	−2.3	−1.46	−0.8	M (0.60), dr	[70]
182	CH$_3$CN	HBF$_4$	−1.6	−0.28	−1.3	S (0.80), dr	[70]
187	CH$_3$CN	Acetic	−1.73	−1.46	−0.27	W (0.16)[c]	[72]
189	CH$_3$CN	Acetic	−2.2	−1.46	−0.7	W (0.19)	[73]
191	CH$_3$CN	CF$_3$COOH	−1.6	−0.89	−0.7	M (0.34)	[74]
191	CH$_3$CN	Acetic	−2.2	−1.46	−0.7	W (0.11)	[74]
192	CH$_3$CN	Acetic	−2.15	−1.46	−0.69	W (0.19)	[75]
193	CH$_3$CN	p-Toluene-sulfonic	−1.5	−0.65	−0.8	M (0.65)	[76]

Table 4.5 (continued)

Compounds	Solvent	Acid	Potential of catalysis (V) vs. Fc$^+$/Fc	$E°_{HA}$ (V) vs. Fc$^+$/Fc	Overpotential (V)	Catalytic efficiency (C.E.)	Reference
194	CH$_3$CN	Acetic	−1.3[d]	−1.46			[77]
195	CH$_3$CN	Acetic	−2.1[e]	−1.46	−0.6	M (0.28), dr	[77a]
199	CH$_3$CN	Acetic	−2.1	−1.46	−0.6	M (0.51)	[77a]
203	CH$_3$CN	Acetic	−1.2[d]	−1.46			[77a]
204	CH$_3$CN	Acetic	−2.2	−1.46	−0.7	M (0.65), dr	[77a]
207	CH$_3$CN	Acetic	−2.3	−1.46	−0.8	M (0.40)	[79]
208	CH$_3$CN	Et$_3$NH$^+$	−1.95	−1.25	−0.70	cnj	[80]
209	CH$_3$CN	4-BrC$_6$H$_4$OH	−2.29	−1.65	−0.64	W (0.21)	[83]
		2-BrC$_6$H$_4$OH	−2.14	−1.55	−0.59	M (0.43)	
		Acetic	−2.11	−1.46	−0.65	M (0.64)	
		Benzoic	−2.08	−1.35	−0.73	S (0.79)	
		Chloroacetic	−2.02	−1.25	−0.77	S (0.96)	
		Cyanoacetic	−1.96	−1.20	−0.76	S (0.94)	
209	CH$_3$CN	Acetic	−2.06	−1.46	−0.60	M (0.31)	[86]
209	CH$_2$Cl$_2$	HBF$_4$	−1.4	−0.28	−1.1	M (0.38)	[20]
209	CH$_3$CN	p-Toluene-sulfonic	−1.25	−0.65	−0.60	W (0.23)	[90]
211	CH$_3$CN	CF$_3$SO$_3$H	−1.18	−0.29	−0.89	M (0.70)	[84]
212	CH$_3$CN	p-Toluene-sulfonic	−1.2	−0.65	−0.6	M (0.27)	[82]
215	CH$_3$CN	CF$_3$SO$_3$H	−1.1[b]	−0.29	−0.8		[84]
220	CH$_3$CN	Acetic	−2.05	−1.46	−0.59	W (0.12)	[86]
222	CH$_3$CN	Acetic	−2.05	−1.46	−0.59	W (0.12)	[86]
223	CH$_3$CN	Acetic	−2.05	−1.46	−0.59	W (0.12)	[86]
224	CH$_3$CN	Acetic	−2.1 (no pk)	−1.46	−0.6	W (0.09)	[86]
225	CH$_3$CN	Acetic	−2.1 (no pk)	−1.46	−0.6	W (0.09)	[86]
226	CH$_3$CN	Acetic	−2.10	−1.46	−0.64	M (0.38)	[86]
228	CH$_3$CN	CF$_3$COOH	−1.48[b]	−0.89	−0.59	M (0.33)	[16]
229	CH$_3$CN	Acetic	−2.06	−1.46	−0.60	M (0.33)	[88]

[a] Potentials are referenced to ferrocene in acetonitrile and correspond to the peak of the catalytic process. Standard potentials are for the HA + 2e$^-$ ⇌ H$_2$ + 2A$^-$ couple in acetonitrile. These were calculated as shown in reference [11] using pK_a-values from the literature except for HBF$_4$ which is assumed to have the same pK_a as H$_3$O$^+$, 2.3, in acetonitrile that has not been rigorously dried [57]. "dr": probably significant contribution from direct reduction of the acid at the working electrode. "cnj": could not judge because the catalytic current appeared to include a significant contribution from acid-promoted reduction of the catalyst, no voltammograms were presented, the catalytic peak was not well resolved from other peaks or any of a number of other reasons. Overpotentials are the catalytic peak potential minus the standard potential. Catalytic efficiency, C.E., is defined in the text, Section 2.4.

[b] May not be catalyzed reduction of acid.

[c] Actual catalyst may be the product of reduction of the nitrophenyl group.

[d] Reduction of the nitro group. Another process near −2 V may be catalyzed reduction of acid.

[e] Current may include reduction of formyl group.

largest value of CEP*. Data for the oxidation potential for three compounds form a line parallel to but lower than the reduction potential correlation. This increased sensitivity of the anodic peak potential to changes in ligand has been discussed above.

Thus, the cathodic and anodic peak potentials are also measures of ligand donor ability and the correlation shown in Fig. 4.1 may be useful in predicting peak potentials for new complexes whose CEP* values have been reported. (There have been other correlations of ligand donor ability with electrochemical parameters. For a review, see [97]. Also see [87] for correlation of CO frequencies with reduction potential for five complexes). It is perhaps surprising that CEP*, based as it is on the A$_1$ v(CO) vibrational frequency in LNi(CO)$_3$, would provide reasonably linear fits for data obtained with these much different Fe$_2$S$_2$ complexes. It is also interesting that a correlation is found in spite of the fact that most of the reported anodic and cathodic processes are irreversible.

4.3. Catalysis of the reduction of acids

About 80 different complexes have been studied with respect to their ability to catalyze the reduction of acids to form hydrogen and the results are summarized in Table 4.5. Reported there are complexes with compound numbers as found in Table 3.1, the solvent (usually acetonitrile), the acid, the peak (or plateau) potentials for the catalytic process, the standard potential for reduction of the acid, the overpotential and catalytic efficiency, C.E., as well as a categorization of the C.E. as weak (W; C.E. < 0.25), medium (M; 0.25 < C.E. < 0.75) and strong (S; C.E. > 0.75). In a few instances, the overpotential is not reported either because the standard potential is not known in the solvent used (THF or CH$_2$Cl$_2$) or because the "catalytic current" may in fact not be due to reduction of the acid but to further reduction of the catalyst in the presence of acid.

Perusal of Table 4.5 will reveal that C.E. ranges from a very small catalytic effect (C.E. = 0.01–0.05) to values around unity. In Section 2.4 where C.E. is defined, it was argued that C.E. = 1 should correspond to such efficient catalysis that the current is limited by the rate of diffusion of the acid to the electrode. There are only nine catalysts that give C.E. categorized as S, i.e., C.E. > 0.75 (**21**, **51**, **52**, **111**, **126**, **149**, **167**, **182**, **209**). Eight of these show strong catalytic efficiency for a single acid while one, **209**, gives C.E. > 0.75 for three different acids. The most common acids that give strong catalysis are quite strong acids: CF$_3$SO$_3$H (**51**, **52**, **126**, **149**), HClO$_4$ (**167**) and HBF$_4$ (**182**). Only two catalysts produce strong catalysis with the weaker acid, acetic acid **21** and **111**. There is no obvious structural feature that is common to all of these nine efficient catalysts.

In terms of overpotential, these nine efficient catalysts have overpotentials ranging from −0.7 V to −1.46 V, i.e., quite large values. Overpotentials as small as −0.2 V have been reported (**14**) but the C.E. is quite small in that case, 0.09. In fact, the catalysts with low overpotential all tend to have small C.E., an interesting exception being **93** with an overpotential of −0.34 V and C.E. in the medium range, 0.40.

To see if there is a correlation between overpotential and C.E. a plot of one against the other was prepared (Fig. 4.2). Clearly, there is only a very weak correlation between the two variables but the aforementioned trends are borne out. That is, efficient catalysts tend to work at large overpotentials and low overpotential is usually associated with weak catalysis. The linear regression line simply indicates that this general trend can be found in the data set.
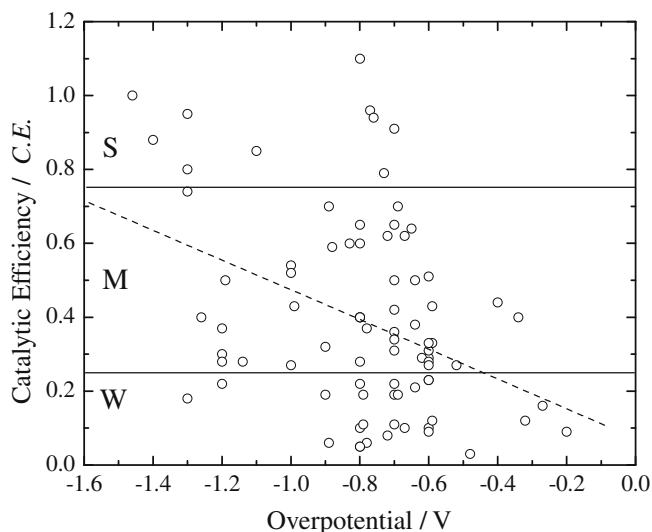
Fig. 4.2. Scatter plot of catalytic efficiency, *C.E.*, vs. overpotential for the catalytic reduction of acids as listed in Table 4.5. *C.E.* categorized as strong (S), medium (M) and weak (W). Dashed line is the linear regression.

The profound scatter in the data can be traced to inadequacies in the concept of *C.E.*: systems that react by completely different mechanisms are being compared; the catalytic peaks of different complexes often have completely different shapes or there is no peak that is evident, only a plateau-like feature; we were unable to correct the data for direct reduction of the acids that is especially important with strong acids at quite negative potentials; etc.

A rationalization of the relationship between efficiency and catalytic peak potential has been presented for a single catalyst **209** with several acids [83] and with a number of structurally related catalysts **220**–**226** and a single acid, acetic acid [84]. In almost all of the mechanisms that have been proposed for catalyzed reduction of acids there are a series of electron-transfer and proton-transfer reactions. The catalysis usually occurs at a potential where the catalyst is reduced from one form to another. Assume that one of the proton-transfers (from weak acid to a reduced form of the catalyst) is rate-determining. Thus, the catalytic efficiency can be enhanced by using a strong acid (which favors this proton-transfer reaction) but this also causes E°_{HA} to be less negative which leads in turn to a larger overpotential. Thus, large *C.E.* and large overpotential go hand-in-hand. Conversely, a weaker acid will bring about a smaller *C.E.* (by suppressing the proton-transfer) but the E°_{HA} will be more negative for that acid, leading to a smaller overpotential.

It would be naïve to think that such an explanation can be even partially valid for all of the catalysts and acids presented in Table 4.5. However, it could provide some guidance in the design of improved catalysts.

Acknowledgements

References

[1] J.W. Peters, W.N. Lanzilotta, B.J. Lemon, L.C. Seefeldt, Science 282 (1998) 1853–1858.
[2] (a) A.J. Bard, L.R. Faulkner, Electrochemical Methods. Fundamentals and Applications, 2nd ed., Wiley, New York, 2001 (Chapter 5);
    (b) D.H. Evans, K.M. O'Connell, R.A. Petersen, M.J. Kelly, J. Chem. Ed. 60 (1983) 290–293.
[3] G. Gritzner, J. Kůta, Pure Appl. Chem. 54 (1982) 1528.
[4] G. Gritzner, J. Kůta, Pure Appl. Chem. 54 (1982) 462.
[5] N. Okumura, D.H. Evans, Unpublished results, University of Arizona, 2006.
[6] Ref. [2], Back flyleaf.
[7] R. Mejia-Rodriguez, D. Chong, J.H. Reibenspies, M.P. Soriaga, M.Y. Darensbourg, J. Am. Chem. Soc. 126 (2004) 12004.
[8] D. Chong, I.P. Georgakaki, R. Mejia-Rodriguez, J. Sanabria-Chincilla, M.P. Soriaga, M.Y. Darensbourg, Dalton Trans. (2003) 4158.
[9] J.W. Tye, J. Lee, H.-W. Wang, R. Mejia-Rodriguez, J.H. Reibenspies, M.B. Hall, M.Y. Darensbourg, Inorg. Chem. 44 (2005) 5550.
[10] Correspondence between D.H. Evans and M.Y. Darensbourg, 2007.
[11] G.A.N. Felton, R.S. Glass, D.L. Lichtenberger, D.H. Evans, Inorg. Chem. 45 (2006) 9181. Corrections: Inorg. Chem. 46 (2007) 5126; 46 (2007) 8098.
[12] G.A.N. Felton, A.K. Vannucci, N. Okumura, L.T. Lockett, D.H. Evans, R.S. Glass, D.L. Lichtenberger, Organometallics 27 (2008) 4671.
[13] R. Mathieu, R. Poilblanc, P. Lemoine, M. Gross, J. Organomet. Chem. 165 (1979) 243.
[14] A. Darchen, H. Mousser, H. Patin, J. Chem. Soc., Chem. Commun. (1988) 968–970.
[15] S.J. Borg, S.K. Ibrahim, C.J. Pickett, S.P. Best, C.R. Chimie 11 (2008) 852–860.
[16] L.-C. Song, J. Cheng, J. Yan, H.-T. Wang, X.-F. Liu, Q.-M. Hu, Organometallics 25 (2006) 1544–1547.
[17] C.M. Thomas, O. Rüdiger, T. Liu, C.E. Carson, M.B. Hall, M.Y. Darensbourg, Organometallics 26 (2007) 3976–3984.
[18] Z. Yu, M. Wang, P. Li, W. Dong, F. Wang, L. Sun, Dalton Trans. (2008) 2400–2406.
[19] Y. Si, M. Hu, C. Chen, C.R. Chimie 11 (2008) 932–937.
[20] J.-F. Capon, F. Gloaguen, P. Schollhammer, J. Talarmin, J. Electroanal. Chem. 566 (2004) 241–247.
[21] L.-C. Song, J. Gao, H.-T. Wang, Y.-J. Hua, H.-T. Fan, X.-G. Zhang, Q.-M. Hu, Organometallics 25 (2006) 5724–5729.
[22] A.K. Justice, M.J. Nilges, T.B. Rauchfuss, S.R. Wilson, L. De Gioia, G. Zampella, J. Am. Chem. Soc. 130 (2008) 5293–5301.
[23] M.T. Olsen, M. Bruschi, L. De Gioia, T.B. Rauchfuss, S.R. Wilson, J. Am. Chem. Soc. 130 (2008) 12021–12030.
[24] A.K. Justice, L. De Gioia, M.J. Nilges, T.B. Rauchfuss, S.R. Wilson, G. Zampella, Inorg. Chem. 47 (2008) 7405–7414.
[25] M. Razavet, S.C. Davies, D.L. Hughes, J.E. Barclay, D.J. Evans, S.A. Fairhurst, X. Liu, C.J. Pickett, Dalton Trans. (2003) 586–595.
[26] P. Li, M. Wang, C. He, G. Li, X. Liu, C. Chen, B. Åkermark, L. Sun, Eur. J. Inorg. Chem. (2005) 2506–2513.
[27] M.-Q. Hu, C.-B. Ma, Y.-T. Si, C.-N. Chen, Q.-T. Liu, J. Inorg. Biochem. 101 (2007) 1370–1375.
[28] L.-C. Song, C.-G. Li, J.-H. Ge, Z.-Y. Yang, H.-T. Wang, J. Zhang, Q.-M. Hu, J. Inorg. Biochem. 102 (2008) 1973–1979.
[29] (a) F. Gloaguen, J.D. Lawrence, M. Schmidt, S.R. Wilson, T.B. Rauchfuss, J. Am. Chem. Soc. 123 (2001) 12518–12527;
    (b) A. Le Cloirec, S.P. Best, S. Borg, S.C. Davies, D.J. Evans, D.L. Hughes, C.J. Pickett, Chem. Commun. (1999) 2285–2286.
[30] L. Duan, M. Wang, P. Li, Y. Na, N. Wang, L. Sun, Dalton Trans. (2007) 1277–1283.
[31] J.-F. Capon, S. Ezzaher, F. Gloaguen, F.Y. Pétillon, P. Schollhammer, J. Talarmin, T.J. Davin, J.E. McGrady, K.W. Muir, New J. Chem. 31 (2007) 2052–2064.
[32] S.J. Borg, T. Behrsing, S.P. Best, M. Razavet, X. Liu, C.J. Pickett, J. Am. Chem. Soc. 126 (2004) 16988–16999.
[33] L.-C. Song, C.-G. Li, J. Gao, B.-S. Yin, X. Luo, X.-G. Zhang, H.-L. Bao, Q.-M. Hu, Inorg. Chem. 47 (2008) 4545–4553.
[34] M.L. Singleton, R.M. Jenkins, C.L. Klemashevich, M.Y. Darensbourg, C.R. Chimie 11 (2008) 861–874.
[35] H. Wolpher, M. Borgström, L. Hammarström, J. Berquist, V. Sundström, S. Styring, L. Sun, B. Åkermark, Inorg. Chem. Commun. 6 (2003) 989–991.
[36] Z. Wang, W. Jiang, J. Liu, W. Jiang, Y. Wang, B. Åkermark, L. Sun, J. Organomet. Chem. 693 (2008) 2828–2834.
[37] D. Morvan, J.-F. Capon, F. Gloaguen, P. Schollhammer, J. Talarmin, Eur. J. Inorg. Chem. (2007) 5062–5068.
[38] F. Gloaguen, J.D. Lawrence, T.B. Rauchfuss, M. Bénard, M.-M. Rohmer, Inorg. Chem. 41 (2002) 6573–6582.
[39] S. Ezzaher, J.-F. Capon, F. Gloaguen, F.Y. Pétillon, P. Schollhammer, J. Talarmin, Inorg. Chem. 48 (2009) 2–4.
[40] P. Li, M. Wang, C. He, X. Liu, K. Jin, L. Sun, Eur. J. Inorg. Chem. (2007) 3718–3727.
[41] Z. Wang, J. Liu, C. He, S. Jiang, B. Åkermark, L. Sun, Inorg. Chim. Acta 360 (2007) 2411–2419.
[42] Y. Na, M. Wang, K. Jin, R. Zhang, L. Sun, J. Organomet. Chem. 691 (2006) 5045–5051.
[43] J. Hou, X. Peng, Z. Zhou, S. Sun, X. Zhao, S. Gao, J. Organomet. Chem. 691 (2006) 4633–4640.
[44] S. Ezzaher, J.-F. Capon, F. Gloaguen, F.Y. Pétillon, P. Schollhammer, J. Talarmin, Inorg. Chem. 46 (2007) 9863–9872.
[45] L. Schwartz, J. Ekström, R. Lomoth, S. Ott, Chem. Commun. (2006) 4206–4208.
[46] F. Gloaguen, J.D. Lawrence, T.B. Rauchfuss, J. Am. Chem. Soc. 123 (2001) 9476–9477.
[47] C.M. Thomas, T. Liu, M.B. Hall, M.Y. Darensbourg, Inorg. Chem. 47 (2008) 7009–7024.

[48] J.-F. Capon, S. El Hassnaoui, F. Gloaguen, P. Schollhammer, J. Talarmin, Organometallics 24 (2005) 2020–2022.
[49] T. Li, M.Y. Darensbourg, J. Am. Chem. Soc. 129 (2007) 7008–7009.
[50] D. Morvan, J.-F. Capon, F. Gloaguen, A. Le Goff, M. Marchivie, F. Michaud, P. Schollhammer, J. Talarmin, J.-J. Yaouanc, R. Pichon, N. Kervarec, Organometallics 26 (2007) 2042–2052.
[51] W. Gao, J. Ekström, J. Liu, C. Chen, L. Eriksson, L. Weng, B. Åkermark, L. Sun, Inorg. Chem. 46 (2007) 1981–1991.
[52] Z. Wang, J.-H. Liu, C.-J. He, S. Jiang, B. Åkermark, L.-C. Sun, J. Organomet. Chem. 692 (2007) 5501–5507.
[53] W. Gao, J. Liu, W. Jiang, M. Wang, L. Weng, B. Åkermark, L. Sun, C.R. Chimie 11 (2008) 915–921.
[54] S. Ezzaher, P.-Y. Orain, J.-F. Capon, F. Gloaguen, F.Y. Pétillon, T. Roisnel, P. Schollhammer, J. Talarmin, Chem. Commun. (2008) 2547–2549.
[55] L.-C. Song, J.-H. Ge, J. Yan, H.-T. Wang, X. Luo, Q.-M. Hu, Eur. J. Inorg. Chem. (2008) 164–171.
[56] Y. Si, C. Ma, M. Hu, H. Chen, C. Chen, Q. Liu, New J. Chem. 31 (2007) 1448–1454.
[57] J.-F. Capon, S. Ezzaher, F. Gloaguen, F.Y. Pétillon, P. Schollhammer, J. Talarmin, Chem. Eur. J. 14 (2008) 1954–1964.
[58] L.-C. Song, B.-S. Yin, Y.-L. Li, L.-Q. Zhao, J.-H. Ge, Z.-Y. Yang, Q.-M. Hu, Organometallics 26 (2007) 4921–4929.
[59] W. Gao, J. Liu, C. Ma, L. Weng, K. Jin, C. Chen, B. Åkermark, L. Sun, Inorg. Chim. Acta 359 (2006) 1071–1080.
[60] Y. Na, M. Wang, J. Pan, P. Zhang, B. Åkermark, L. Sun, Inorg. Chem. 47 (2008) 2805–2810.
[61] L. Schwartz, G. Eilers, L. Eriksson, A. Gogoll, R. Lomoth, S. Ott, Chem. Commun. (2006) 520–522.
[62] G. Eilers, L. Schwartz, M. Stein, G. Zampella, L. de Gioia, S. Ott, R. Lomoth, Chem. Eur. J. 13 (2007) 7075–7084.
[63] F. Wang, M. Wang, X. Liu, K. Jin, W. Dong, L. Sun, Dalton Trans. (2007) 3812–3819.
[64] S. Ott, M. Kritikos, B. Åkermark, L. Sun, R. Lomoth, Angew. Chem., Int. Ed. 43 (2004) 1006–1009.
[65] S. Jiang, J. Liu, L. Sun, Inorg. Chem. Commun. 9 (2006) 290–292.
[66] S. Jiang, J. Liu, Y. Shi, Z. Wang, B. Åkermark, L. Sun, Polyhedron 26 (2007) 1499–1504.
[67] S. Jiang, J. Liu, Y. Shi, Z. Wang, B. Åkermark, L. Sun, Dalton Trans. (2007) 896–902.
[68] L.-C. Song, L.-X. Wang, B.-S. Yin, Y.-L. Li, X.-G. Zhang, Y.-W. Zhang, X. Luo, Q.-M. Hu, Eur. J. Inorg. Chem. (2008) 291–297.
[69] J. Hou, X. Peng, J. Liu, Y. Gao, X. Zhao, S. Gao, K. Han, Eur. J. Inorg. Chem. (2006) 4679–4686.
[70] W.-G. Wang, H.-Y. Wang, G. Si, C.-H. Tung, L.-Z. Wu, Dalton Trans. (2009) 2712–2720.
[71] S. Ott, M. Borgström, M. Kritikos, R. Lomoth, J. Bergquist, B. Åkermark, L. Hammarström, L. Sun, Inorg. Chem. 43 (2004) 4683–4692.
[72] T. Liu, M. Wang, Z. Shi, H. Cui, W. Dong, J. Chen, B. Åkermark, L. Sun, Chem. Eur. J. 10 (2004) 4474–4479.
[73] L.-C. Song, J.-H. Ge, X.-G. Zhang, Y. Liu, Q.-M. Hu, Eur. J. Inorg. Chem. (2006) 3204–3210.
[74] L.-C. Song, J.-H. Ge, X.-F. Liu, L.-Q. Zhao, Q.-M. Hu, J. Organomet. Chem. 691 (2006) 5701–5709.
[75] L.-C. Song, H.-T. Wang, J.-H. Ge, S.-Z. Mei, J. Gao, L.-X. Wang, B. Gai, L.-Q. Zhao, J. Yan, Y.-Z. Wang, Organometallics 27 (2008) 1409–1416.
[76] V. Vijaikanth, J.-F. Capon, F. Gloaguen, F.Y. Pétillon, P. Schollhammer, J. Talarmin, J. Organomet. Chem. 692 (2007) 4177–4181.
[77] (a) G. Si, W.-G. Wang, H.-Y. Wang, C.-H. Tung, L.-Z. Wu, Inorg. Chem. 47 (2008) 8101–8111;
(b) G. Si, W.-G. Wang, J. Ding, X.-F. Shan, Y.-P. Zhao, C.-H. Tung, M. Xu, Tetrahedron Lett. 48 (2007) 4775–4779.
[78] H. Cui, M. Wang, L. Duan, L. Sun, J. Coord. Chem. 61 (2008) 1856–1861.
[79] L.-C. Song, Z.-Y. Yang, H.-Z. Bian, Y. Liu, H.-T. Wang, X.-F. Liu, Q.-M. Hu, Organometallics 24 (2005) 6126–6135.
[80] L.-C. Song, Z.-Y. Yang, Y.-J. Hua, H.-T. Wang, Y. Liu, Q.-M. Hu, Organometallics 26 (2007) 2106–2110.
[81] J. Windhager, M. Rudolph, S. Bräutigam, H. Görls, W. Weigand, Eur. J. Inorg. Chem. (2007) 2748–2760.
[82] F. Gloaguen, D. Morvan, J.-F. Capon, P. Schollhammer, J. Talarmin, J. Electroanal. Chem. 603 (2007) 15–20.
[83] G.A.N. Felton, A.K. Vannucci, J. Chen, L.T. Lockett, N. Okumura, B.J. Petro, U.I. Zakai, D.H. Evans, R.S. Glass, D.L. Lichtenberger, J. Am. Chem. Soc. 129 (2007) 12521–12530.
[84] L. Schwartz, P.S. Singh, L. Eriksson, R. Lomoth, S. Ott, C.R. Chimie 11 (2008) 875–889.
[85] R.D. Adams, S. Miao, Inorg. Chem. 43 (2004) 8414–8426.
[86] J. Chen, C.A. Mebi, N. Okumura, A.K. Vannucci, U.I. Zakai, D.L. Lichtenberger, D.H. Evans, R.S. Glass, submitted for publication.
[87] L. Schwartz, L. Eriksson, R. Lomoth, F. Teixdor, C. Viñas, S. Ott, Dalton Trans. (2008) 2379–2381.
[88] P. Li, M. Wang, J. Pan, L. Chen, N. Wang, L. Sun, J. Inorg. Biochem. 102 (2008) 952–959.
[89] S. Gao, J. Fan, S. Sun, X. Peng, X. Zhao, J. Hou, Dalton Trans. (2008) 2135–2185.
[90] J.-F. Capon, F. Gloaguen, P. Schollhammer, J. Talarmin, J. Electroanal. Chem. 595 (2006) 47–52.
[91] R.H. Crabtree, The Organometallic Chemistry of the Transition Metals, 4th ed., Wiley, New York, 2005.
[92] S. Ezzaher, J.-F. Capon, F. Gloaguen, F.Y. Pétillon, P. Schollhammer, J. Talarmin, Inorg. Chem. 46 (2007) 3426–3428.
[93] A.K. Justice, G. Zampella, L. De Gioia, T.B. Rauchfuss, J.I. van der Vlugt, S.R. Wilson, Inorg. Chem. 46 (2007) 1655–1664.
[94] M.L. Singleton, N. Bhuvanesh, J.H. Reibenspies, M.Y. Darensbourg, Angew. Chem., Int. Ed. 47 (2008) 9492–9495.
[95] J.-F. Capon, F. Gloaguen, F.Y. Pétillon, P. Schollhammer, J. Talarmin, C.R. Chimie 11 (2008) 842–851.
[96] L. Perrin, E. Clot, O. Eisenstein, J. Loch, R.H. Crabtree, Inorg. Chem. 40 (2001) 5806–5811.
[97] A.J.L. Pombeiro, Eur. J. Inorg. Chem. (2007) 1473–1482.
[98] U.-P. Apfel, Y. Halpin, M. Gottschaldt, H. Görls, J.G. Vos, W. Weigand, Eur. J. Inorg. Chem. (2008) 5112–5118.
[99] J.-F. Capon, F. Gloaguen, F.Y. Pétillon, P. Schollhammer, J. Talarmin, Coord. Chem. Rev., doi:10.1016/j.ccr.2008.10.020.